Report
P-17-08
August 2018

Modelling the interaction between engineered and natural barriers in BRIE

Task 8 of SKB Task Forces EBS and GWFTS

Ilona Hancilova
Milan Hokr

SVENSK KÄRNBRÄNSLEHANTERING AB

SWEDISH NUCLEAR FUEL
AND WASTE MANAGEMENT CO

Box 3091, SE-169 03 Solna
Phone +46 8 459 84 00
skb.se

SVENSK KÄRNBRÄNSLEHANTERING

ISSN 1651-4416
SKB P-17-08
ID 1673658
August 2018

Modelling the interaction between engineered and natural barriers in BRIE

Task 8 of SKB Task Forces EBS and GWFTS

Ilona Hancilova, Milan Hokr
Technical University of Liberec

Executive summary

We solve selected subtasks of Task 8 connected with bentonite hydration using alternative model conception. Considered approach represents usually used Richards' equation for flow in partly saturated conditions in the form of diffusion equation with nonlinear diffusivity. This approach has some limitations connected with degree of saturation as a dependent variable which will be described in following chapters. Problems are solved with commercial simulation tool Ansys (ANSYS 2010) through the heat transfer equation which is analogous to the diffusion equation.

We focused on obtaining qualitative and partly quantitative information about bentonite hydration within BRIE experiment using alternative modelling approach and available measured data. We also want to show the degree of correspondence of the model results with measured data when it is used simplified model geometry.

Sammanfattning

Vi löser utvalda delområden av modelleringsuppgift Task 8 som är kopplade till bentonithydratisering med alternativa modellkoncept. Vald metod representerar vanligtvis Richards ekvation för flöde under delvis mättade förhållanden i form av diffusionsekvation med olinjär diffusivitet. Detta tillvägagångssätt har vissa begränsningar kopplade till mättnadsgraden som en beroende variabel vilket kommer att beskrivas i de följande kapitlen. Problemen löstes med det kommersiella simuleringsverktyget Ansys (ANSYS 2010) med hjälp av värmeöverföringsekvationen som är analog med diffusionsekvationen.

Vi fokuserade på att erhålla kvalitativ och delvis kvantitativ information om bentonithydratisering inom BRIE-experimentet med hjälp av en alternativ modelleringsmetod och tillgängliga uppmätta data. Vi vill också visa på graden av överensstämmelse för modellresultaten med uppmätta data när metoden används med förenklad modellgeometri.

Contents

1 Introduction

1.1 Background

Nuclear waste program in the Czech Republic is based on Swedish deposition method KBS-3V – spent nuclear fuel in special canisters places deeply in crystalline rock and sealed with bentonite barrier.

1.2 Objectives

The main objectives are the same as general objectives listed in Task 8 definition – understanding of the processes in the bentonite barrier and at the rock-bentonite interface too. Next goal is to model the process of bentonite hydration using alternative approach (diffusion equation in our case).

1.3 Scope

We simulated selected subtasks of Task 8:

1. **The pilot simulation of inflow** into the borehole as a sensitivity analysis in simplified case as a flow in saturated conditions – different model conception and solution with different simulation tool – **Chapter 2**.
2. Initial scoping calculation within **Task 8a – Chapter 3**.
3. Prediction **Task 8d** of wetting within boreholes of BRIE experiment – **Chapter 4**.
4. **Solution of Task 8d** (comparison of results of modified BRIE models with measured data) – **Chapter 5**.
5. Additional information of **Water Uptake Test** modelling – brief description and results in Appendix 1.

Subtasks Task 8b and Task 8c were not possible to simulate with our modelling tools due to limitations which are in following two points:

- It is not possible to distinguish the state when degree of saturation is equal to 1 for approach with diffusion equation – we consider that rock is fully saturated (The state variable in diffusion equation is degree of saturation and due to this fact it is not possible to distinguish different positive pressure levels in the rock. Inspite that is higher value of pressure in the rock we are able to prescribe full saturation only – which represents all positive pressure levels in our conception.)
- It is not possible to include proportionally smaller boreholes with fractures in 3D geometry with the tunnels in surrounding rock (according to Task 8c and partly Task 8d).

2 Initial calculation – fracture inflow (parametric study)

2.1 Objectives

This problem is a pilot calculation – sensitivity study of free inflow of the water from the fracture to the borehole. We consider flow in saturated conditions which enables the first insight into the problem, further calculations build on referred solutions – but they are simulated as a flow in partly saturated conditions.

2.2 Approach

Problem is solved in software Flow123D developed at Technical University of Liberec which is based on mixed-hybrid formulation of finite element method. Flow123D uses so called "multidimensional concept" which enables using of surface representation of the fracture (2D elements) together with 3D elements as a rock matrix.

2.3 Model setup

Problem is solved as 2D model (model geometry is shown right in Figure 2-1 – fracture is pink, rock is yellow and orange – both domains with the same properties and borehole and tunnel are blue). Fracture is represented by a line – discrete fracture which corresponds to the multi-dimensional Flow123D concept.

Thus our model consists of 2D elements which represent rock and a line (1D object) which represents fracture (Figure 2-1). In Flow123D is not possible to solve axisymmetric problems – the geometry considers infinitely long tunnel with the cross-section of referred profile (not traditional geometry which originated by a rotation of referred profile). Results of the study are used to sensitivity analysis (despite the fact that they do not qualitatively coincide with axisymmetric case) – we are able to compare the amount of inflowing water through the fracture and through the surrounding rock depending on the ratio of hydraulic conductivity or transmissivity respectively.

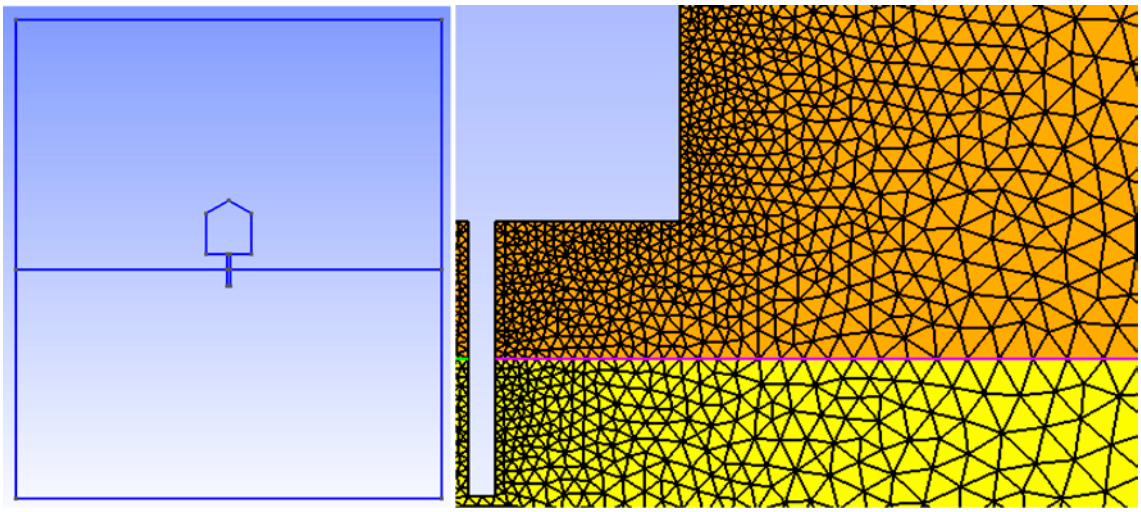

Figure 2-1. *Model geometry and discretization for the problem of the inflow into the borehole.*

Different combinations of hydraulic conductivity of the rock and fracture transmissivity are considered and referred in Table 2-1 and Table 2-2 (together with results). Some combinations express higher or lower values of inflow into the borehole and some of them express higher contrast between inflow through the fracture and through the rock. Selected variants are differentiated by colour: yellow – reference case, green – low value of fracture transmissivity and high value of hydraulic conductivity of the rock and blue – high value of fracture transmissivity and low value of hydraulic conductivity of the rock. The problem with homogeneous rock without the fracture is included as a limit case (solved as a problem with very low value of fracture transmissivity. The model behaves as in the case without fracture. And there is no overflow between 1D (fracture) and 2D (rock) in multidimensional conception).

Table 2-1. Inflows through the fracture into the borehole for different hydraulic parameters of the rock and fracture.

		Fracture transmissivity [$m^2 \times s^{-1}$]			
		1.00×10^{-29} (without the fracture)	**1.00×10^{-12}**	**5.00×10^{-10}**	**1.00×10^{-8}**
Hydraulic conductivity of the rock [$m \times s^{-1}$]	1.00×10^{-14}	1.05×10^{-34}	2.04×10^{-11}	9.57×10^{-10}	1.91×10^{-6}
	1.00×10^{-13}	1.07×10^{-34}	2.57×10^{-11}	9.59×10^{-9}	1.91×10^{-7}
	1.00×10^{-12}	1.07×10^{-34}	3.26×10^{-11}	9.70×10^{-9}	1.92×10^{-7}
	1.00×10^{-11}	1.07×10^{-34}	3.52×10^{-11}	1.07×10^{-8}	1.93×10^{-7}

Table 2-2. Inflows through the rock into the borehole for different hydraulic parameters of the rock and fracture.

		Fracture transmissivity [$m^2 \times s^{-1}$]			
		1.00×10^{-29} (without the fracture)	**1.00×10^{-12}**	**5.00×10^{-10}**	**1.00×10^{-8}**
Hydraulic conductivity of the rock [$m \times s^{-1}$]	1.00×10^{-14}	5.72×10^{-12}	4.79×10^{-12}	2.17×10^{-12}	1.14×10^{-10}
	1.00×10^{-13}	5.77×10^{-11}	5.23×10^{-11}	4.58×10^{-11}	1.47×10^{-11}
	1.00×10^{-12}	5.78×10^{-10}	5.66×10^{-10}	4.70×10^{-10}	4.78×10^{-10}
	1.00×10^{-11}	5.78×10^{-9}	5.76×10^{-9}	4.88×10^{-9}	4.69×10^{-9}

2.4 Results

Results are represented by pressure field and velocity arrows over the model geometry (Figure 2-3) and also by values of the individual inflows through the fracture and through the rock which are summarized in Table 2-1 and Table 2-2.

2.5 Discussion

It is obvious that transmissivity of the fracture has dominant influence on the flow through the fracture and this flow is slightly affected by the rock hydraulic conductivity. (And similarly for the rock: Flow through the rock is mainly influenced by the rock hydraulic conductivity and slightly affected by the fracture transmissivity).

This small influence is possible to explain as a hydraulic interaction between the rock and the fracture (we assume that occurs the water exchange between both entities). In Figure 2-2 is shown uniform increase of the flux dependent on hydraulic conductivity increase. The influence of referred parameter (fracture or rock) is expresses for the reference value of the second parameter.

Figure 2-3 shows the influence of permeable fracture on the pressure field – version with more permeable fracture and less permeable rock (blue cell of the table). It is obvious forces pressure gradient in the fracture which differs from natural pressure field of the rock. And pressure field is uniform in all directions in the version with less permeable fracture (green cell of the table).

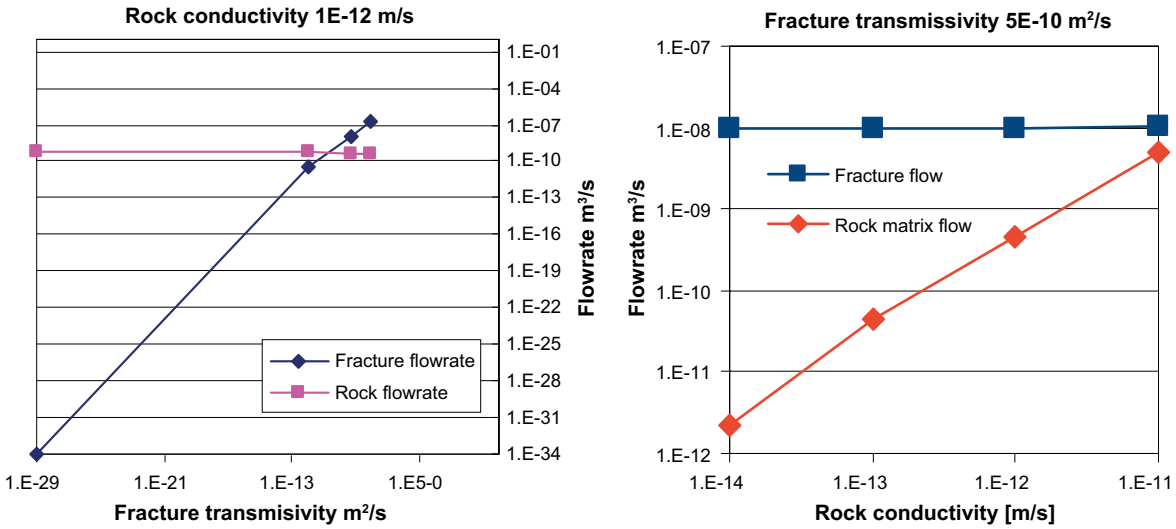

Figure 2-2. *Results of the parametric study – LEFT: influence of the fracture transmissivity on the inflow (fixed value of rock hydraulic conductivity), RIGHT: influence of the rock hydraulic conductivity (fixed value of fracture transmissivity)*

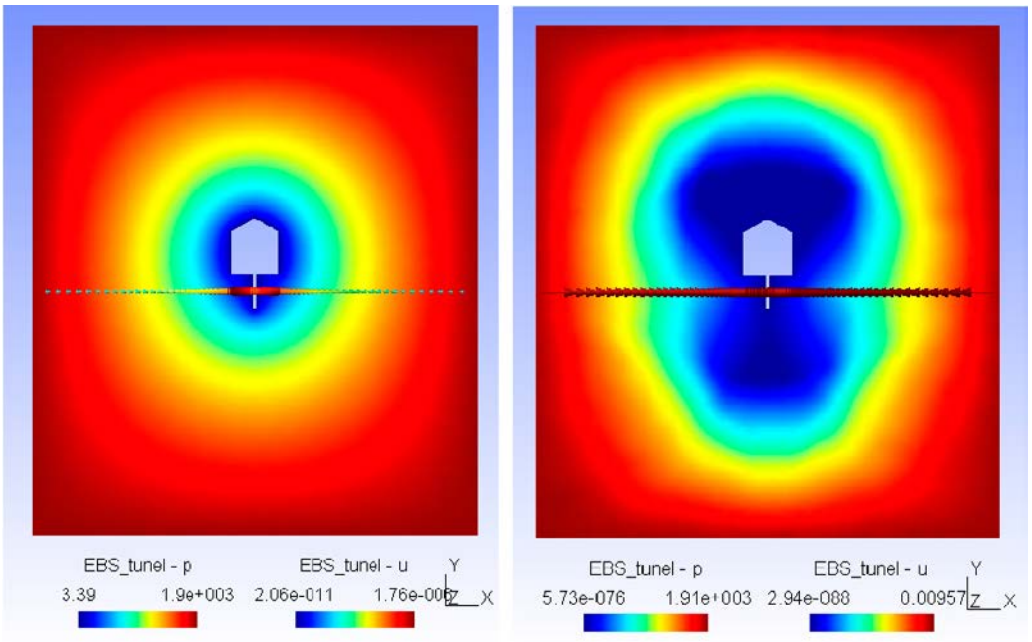

Figure 2-3. *Illustrative examples of the results – pressure fields (colour scale) and velocities (arrows) dependent on hydraulic conditions of the rock and fracture (LEFT picture corresponds with green cells of the tables, RIGHT picture corresponds with blue cells of the tables)*

2.6 Conclusions and recommendations

This problem was solved as a pilot calculation – sensitivity study of free inflow of the water from the fracture into the borehole. This study simplified the insight into the problem and it showed the influence of individual hydraulic parameters on the inflow into the borehole.

3 Task 8a – initial – scoping calculation

3.1 Objectives

This task with initial calculation serves to introduction to the problem and also to testing our computing tool (multiphysical simulation system Ansys) for the problem of bentonite saturation.

3.2 Approach

Bentonite hydration is considered as flow in partly saturated conditions described as diffusion equation in our models. This approach is expressed by the transformation of Richards' equation to diffusion equation with nonlinear diffusivity dependent on degree of saturation according to Börgesson (1985). This alternative formulation expresses the same process as Richards' equation but it has one small limitation – it is not possible to distinguish the behaviour at the state of full saturation (different non-negative pressure levels are represented by a single value of degree of saturation – 100 %). But this limitation is not so important if we are interested in the changes in bentonite saturation and different pressure levels in rock are not in the main sphere of interest. It is necessary to consider this limitation but we try to solve this kind of problems using conception with non-linear diffusion equation to estimate the applicability and usefulness of this method in comparison with more complex methods.

Following text describes initial relation – Darcy's law for flow in partly saturated conditions and final phase of derivation – diffusion equation with nonlinear diffusivity.

$$\bar{q} = -\frac{k \cdot k_r}{\mu}\left(\nabla P_l - \rho_w \cdot \bar{g}\right)$$

$$\kappa \frac{\partial P_l}{\partial t} - \nabla \cdot \bar{q} = Q$$

where $\bar{q}$ is Darcy's velocity, k is a permeability, μ is a dynamic viscosity, P_l is a liquid water pressure, $\tilde{n}_w$ is water density, $\bar{g}$ is acceleration of gravity, ê is a specific storativity, Q sources, and k_r is a relative permeability, which is expressed by permeability ratio for saturated and unsaturated conditions.

Relative permeability is represented by power law for bentonite (relative permeability depends on degree of saturation S_l). Parameter value δ = 3 is considered for bentonite according to Vidstrand et al. (2017)

$$k_r\left(S_l\right) = \left(S_l\right)^{\delta}.$$

Relative permeability for rock is considered according to van Genuchten representation, where λ is van Genuchten retention curve parameter.

$$k_r\left(S_l\right) = \sqrt{S_l}\left(1 - \left(1 - S_l^{\frac{1}{\lambda}}\right)^{\lambda}\right)^2$$

For derivation is also necessary to know retention curve which expresses an ability of the medium to retain the water at different values of water content. We use van Genuchten retention curve with parameters P_0 and λ and atmospheric pressure P_g in the following form.

$$S_l(P_l) = \left(1 + \left(\frac{P_g - P_l}{P_0}\right)^{\frac{1}{1-\lambda}}\right)^{-\lambda} \quad \left(P_l < P_g\right)$$

Diffusion equation is described by following relation where S_l (degree of saturation) is unknown.

$$\frac{\partial S_l}{\partial t} = \nabla \cdot (\nabla D(S_l))$$

Diffusivity of bentonite D_b (S_l) is derived in accordance with following steps referred in Vidstrand et al. (2017).

$$D_b(S_l) = \frac{k \cdot k_r(S_l)}{n \cdot \mu} \cdot \frac{dP_l}{dS_l} = \frac{k}{n \cdot \mu} \cdot S_l^{\,3} dP(S_l) \qquad (\mathrm{m}^2/\mathrm{s})$$

We determined a derivative of an inversion to van Genuchten retention curve.

$$P(S_l) = P_g - P_0 \left(S_l^{\frac{-1}{\lambda}} - 1 \right)^{1-\lambda}$$

$$dP(S_l) = \frac{d}{dS_l} P(S_l) = \frac{P_0}{\lambda} \cdot (1-\lambda) \cdot \left(S_l^{-\frac{1}{\lambda}} - 1 \right)^{-\lambda} \cdot S_l^{\frac{-1-\lambda}{\lambda}}$$

And obtained derivative was put into the relation for diffusivity which depends on degree of saturation as well as retention curve and power law for relative permeability.

$$D_b(S_l) = \frac{k}{n \cdot \mu} \cdot S_l^{\,3} \cdot \frac{P_0}{\lambda} \cdot (1-\lambda) \cdot \left(S_l^{-\frac{1}{\lambda}} - 1 \right)^{-\lambda} \cdot S_l^{\frac{-1-\lambda}{\lambda}}$$

Determination of diffusivity for rock D_r (S_l) is analogical but we used van Genuchten retention curve for the expression of relative permeability depending on degree of saturation according to Vidstrand et al. (2017). Diffusivity for the rock is expressed as

$$D_r(S_l) = \frac{k}{n \cdot \mu} \cdot \sqrt{S_l} \cdot \left(1 - \left(1 - S_l^{\frac{1}{\lambda}} \right)^{\lambda} \right)^2 \cdot \frac{P_0}{\lambda} \cdot (1-\lambda) \cdot \left(S_l^{-\frac{1}{\lambda}} - 1 \right)^{-\lambda} \cdot S_l^{\frac{-1-\lambda}{\lambda}}$$

Models are solved in multiphysical commercial computational tool Ansys. For simulation of diffusion process is used predefined analogical equation for heat transfer – degree of saturation is represented by temperature and diffusivity is represented by this form: $\frac{\lambda}{\mathrm{cp}}$ where λ is heat conductivity, ρ is a density and C is a specific heat capacity).

3.3 Model setup

We solve problems with simple 2D axisymmetric geometry of the borehole with surrounding rock matrix with one horizontal fracture. But we started with initial calculations which were performed on 1D and 2D geometries (model geometry with appropriate dimensions are referred in Figure 3-1 and computational meshes for mentioned models in Figure 3-2). Simple geometry contains either cylindrical borehole consists of bentonite or mentioned borehole with surrounding rock with the tunnel (as an empty space) and one horizontal fracture (material with a high value of permeability). Described problems were solved due to the verification of models functionality and also due to calibration of material parameters.

Values of material parameters, used for the determination of diffusivities of bentonite and rock and fracture, were chosen according to Vidstrand et al. (2017) but we modify the values of permeability in accordance with reference calibration performed on 1D and 2D axisymmetric models (We used data from initial scoping calculations in the Task 8 definition document). Parameter values are referred in Table 3-1 and dependency of diffusivity on degree of saturation in Figure 3-3.

We consider fully saturated rock and fracture at the beginning of the process (S = 1) and initial saturation of bentonite equals to 36 % (S = 0.36). There is prescribed no-flow boundary condition on the bottom of the tunnel and full saturation on the inner model boundaries (unlimited source of water). On the remaining part of the surface of the tunnel is prescribed low value of saturation (S = 0.05).

Table 3-1. Material parameters used for diffusivity determination, parameters according to Vidstrand et al. (2017), column "modified" contains alternative values of permeability, which were obtained during the calibration.

	P_0 [MPa]	λ [1]	$k_{recommended}$ [m^2]	$k_{modified}$ [m^2]	n [1]	μ [Pa × s]
Bentonite	9.23	0.3	6.4×10^{-21}	9.5×10^{-21}	0.438	10^{-3}
Rock	1.74	0.6	6.0×10^{-20}	9.0×10^{-22}	0.003	10^{-3}
Fracture	1.74	0.6	2.5×10^{-15}	2.5×10^{-15}	0.003	10^{-3}

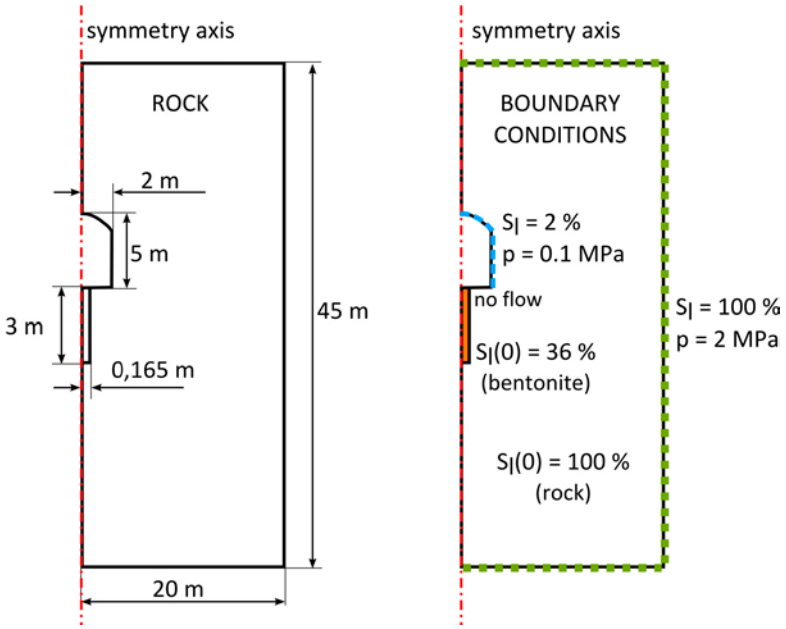

Figure 3-1. *Model geometry of 2D axisymmetric problem with the borehole, surrounding rock and horizontal fracture and used boundary conditions for the same model*

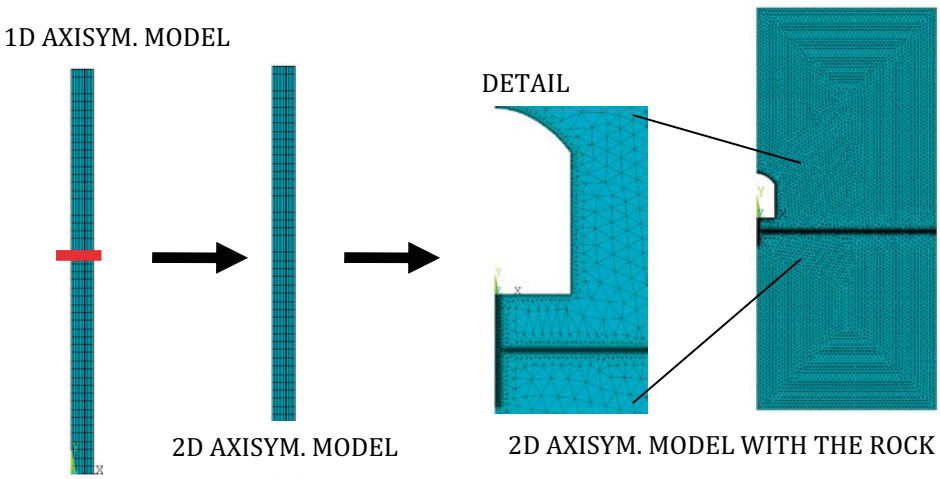

Figure 3-2. *Individual meshes for solved problems, 1D axisymmetric model, 2D axisymmetric model and 2D axisymmetric model with the rock and horizontal fracture.*

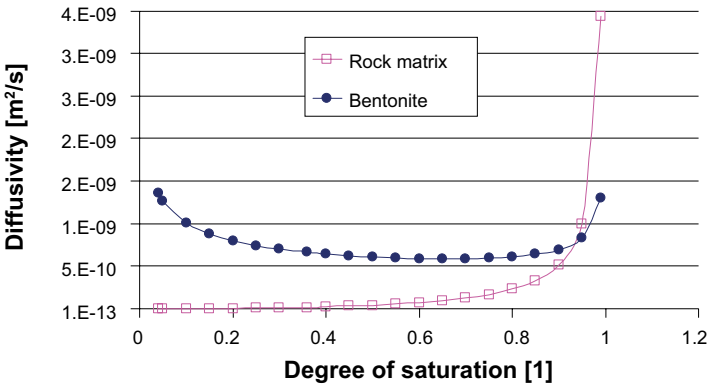

Figure 3-3. *Diffusivity of rock matrix and bentonite dependent on degree of saturation, distributions were determined using modified parameters according to Table 3-1.*

3.4 Results

We obtain the distributions of degree of saturation along the borehole axis as well as along the transverse profile at the height of the fracture. We are able to compare individual profiles over time too and to determine the times of achievement specific degrees of saturation according to our model.

The first problem is 1D axisymmetric model with point inflow without any other influence. This simulation was performed due to model testing and the results were compared with analytical reference computation referred in Vidstrand et al. (2017). They were computed using Darcy's law in partly saturated conditions. Our results (obtained using diffusion equation) showed good correspondence with reference results. The differences in results were quite negligible but it was also problematic to evaluate them because the analytic solution data were plotted in quite coarse resolution.

The second case was 2D axisymmetric model of borehole filled with bentonite without the influence of the surrounding rock with point inflow. This model was also used as a testing case for initial computation and to obtain the basic overview of the process and information about range of bentonite hydration over time.

Model was defined in accordance with the 2D axisymmetric model with the rock (but it was considered bentonite in the borehole only). It was prescribed full saturation on the part of the boundary which was common for the fracture and for the bentonite. It represents unlimited source of water supplied by the fracture. On the rest of the boundary it was prescribed no-flow boundary condition. Results of this model in comparison with results of model with surrounding rock should describe the influence on the profiles of degree of saturation over time (differences in the spatial and time distribution of degree of saturation). The error caused by the neglecting surrounding rock largely depends on the properties of the rock (and fracture too).

The final variant of the model is 2D axisymmetric model of the borehole with bentonite with the rock matrix and fracture which represents the main path for transport of water to bentonite. Unlike the previous case bentonite is hydrated not only through the fracture but also across the rock-bentonite interface. Radial and axial distributions of degree of saturation over time for mentioned model are shown in Figure 3-4 and Figure 3-5 .

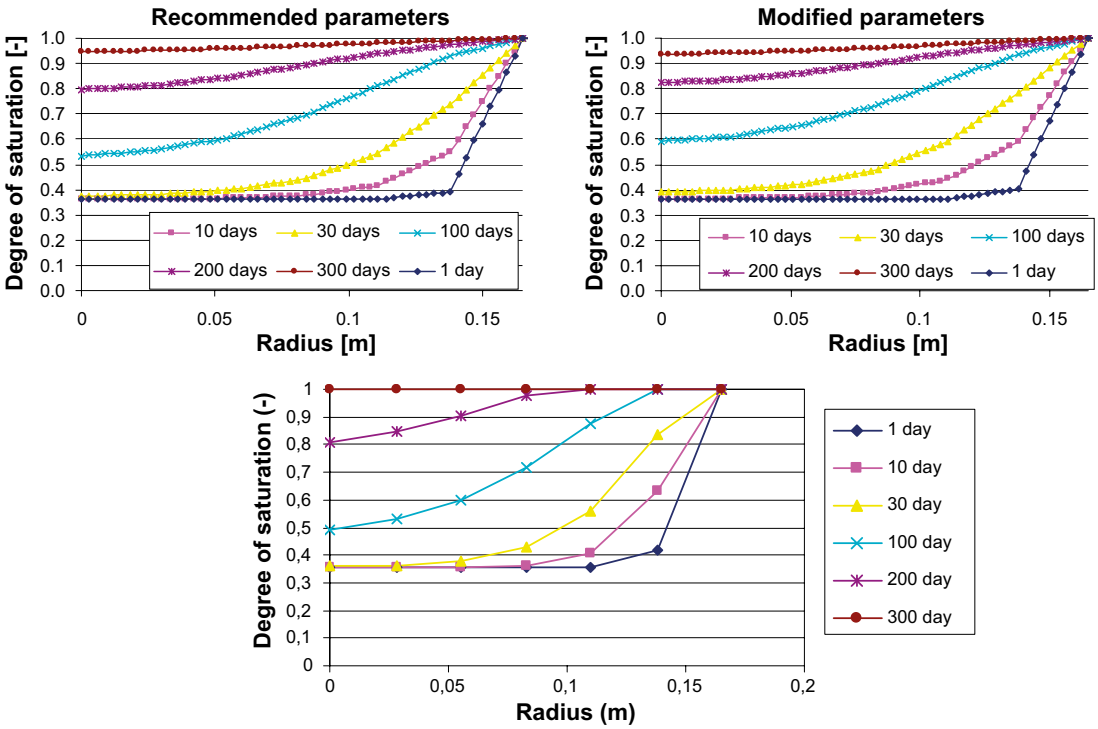

Figure 3-4. *Radial distribution of saturation for 2D axisymmetric model of bentonite with rock, ABOVE: our results (diffusion equation) for recommended and modified parameters for diffusivity determination compared to results BELOW: Code_Bright (Darcy's law for partly saturated conditions referred in Vidstrand et al. (2017))*[1].

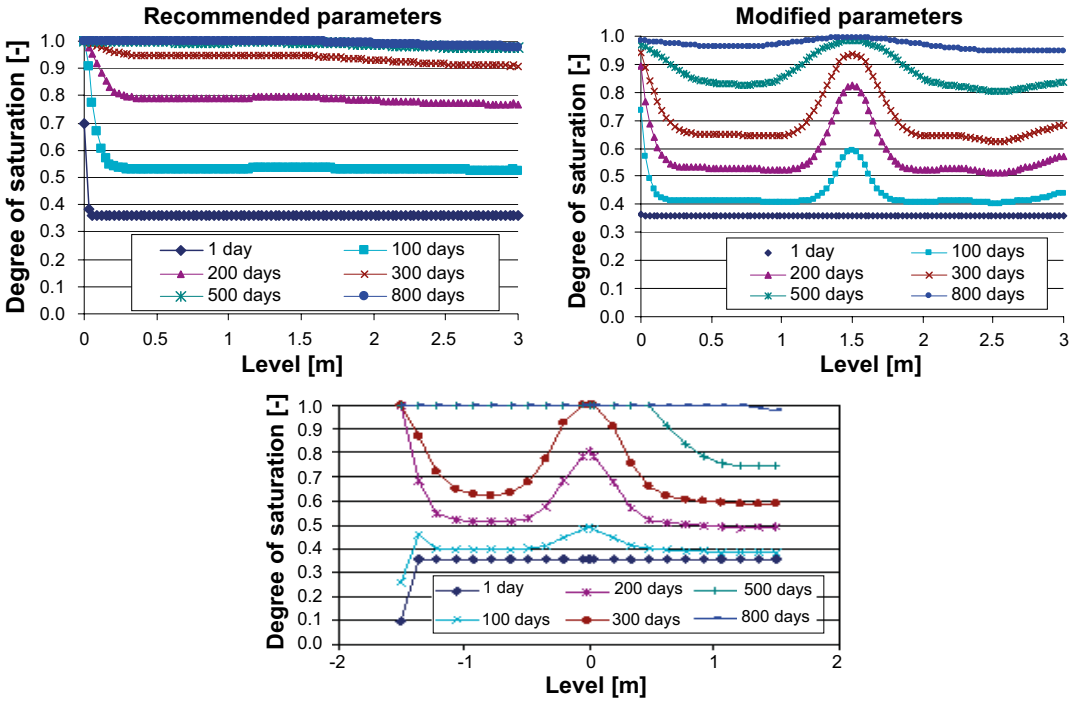

Figure 3-5. *Axial distribution of saturation for 2D axisymmetric model of bentonite with rock, ABOVE: our results (diffusion equation) for recommended and modified parameters for diffusivity determination compared to results BELOW: Code_Bright (Darcy's law for partly saturated conditions referred in Vidstrand et al. (2017))*[2].

[1] "Recommended parameters" are suggested values used in the scoping calculations in Task 8 definition and "modified parameters" are our values of the parameters which were fitted within the solution described in Section 3-3.

[2] Ibid.

3.5 Discussion

Distributions of degree of saturation in Figure 3-4 and Figure 3-5 show that bentonite is almost fully saturated at the time of 800 days.

Radial distributions of degree of saturation for the 2D axisymmetric model of bentonite with rock for recommended and modified[1] material parameters (Figure 3-4) do not show big differences. But according to axial distributions it is possible to say that models with recommended parameters show high influence of hydration through the rock-bentonite interface. Hydration through the fractures is almost unnoticeable. Thus it was necessary to change the parameter values to enforce the influence of the fracture. We set 67times lower value of the rock permeability and 1.5 times higher value of bentonite permeability, parameters of fracture was kept the same. Modified parameters were use in the next simulation and we are able to compare these results with Code_Bright results (Vidstrand et al. 2017). Unfortunately, we have not been able to detect the mistake in our representation of the surrounding rock as a boundary condition so far. But we can add some findings:

- Error is in the representation of the rock because models without rock influence (bentonite only) show good correspondence with Code_Bright and analytical results.
- Some problem is also caused by the simplification of pressure conditions in the rock (we have to set full saturation in the rock which corresponds to the all non-negative pressure levels).
- Current boundary condition expresses the influence of the rock with different permeability.
- It requires additional comparative models.

New distributions obtained from solution with modified parameters qualitatively correspond with Code_Bright results. The differences are evident for axial distributions – our results show that hydration is slower for higher values of degree of saturation in our models compared with Code_Bright results. But the difference is at most 7 % at the final time of 800 days.

3.6 Conclusions and recommendations

Solved models helped us to become familiar with the problems of bentonite saturation. We compared results of the models with scoping calculations in Code_Bright with good correspondence but it was necessary to modify some values of recommended material parameters in Vidstrand et al. (2017) – specifically increase the values of bentonite and rock permeability.

4 Task 8d – BRIE – prediction of wetting

4.1 Objectives

This task describes the process of bentonite wetting for models with simple geometry which takes into account detailed distributions of the fractures present in the rock. Two different distributions of fractures are considered (according to definition of Task 8c and corrected data according to Task 8d definition).

We also observe the evolution of the hydration process of bentonite in the borehole and the influence of the hydration through the fractures and through the rock-bentonite interface and differences between them.

4.2 Approach

We used the same approach in this Task 8d as described for Task 8a – solution with diffusion equation with nonlinear diffusivity simulated in modelling system Ansys.

But there are some differences in the representation of the influence of the fractures and rock-bentonite interface on the hydration process. Fractures and rock are not components of the model – we consider their influence only, through the boundary conditions.

The influence of the fractures is represented by Dirichlet's boundary condition (full saturation – unlimited source of water) prescribed on lines which represent an intersection of the fracture planes with the surface of the borehole.

The influence of surrounding rock is expressed by boundary condition prescribed on the surface of the borehole (except lines mentioned above). Values of this b.c. are estimated from large-scaled 2D axisymmetric model with the surrounding rock without fracture. We used the dependency of flux on degree of saturation – reached flux values at various degrees of saturation of bentonite (at the rock-bentonite interface).

4.3 Model setup

We consider several different versions of referred model. Models differ in the number of fractures and also in the way of the bentonite saturation. Bentonite is hydrated through the fractures only or through the fractures and rock-bentonite interface (we consider two different permeabilities for surrounding rock, called rock_1 and rock_2). In addition fractures are used in two possibilities: several fractures according to Task 8c definition and one present fracture in each borehole according to Task 8d definition. Solved model variants are summarized in Table 4-1.

Table 4-1. Solved variants of models of Task 8d, basic difference is in the number of fractures and also in the influence of the rock on bentonite hydration.

	Borehole	Without rock influence	With rock influence	
			rock_1	rock_2
Several fractures	KO0017G01	✓	✓	✓
(Task 8c definition)	KO0018G01	✓	✓	✓
One fracture	KO0017G01	✓	✓	✓
(Task 8d definition)	KO0018G01	✓	✓	✓

4.4 Model geometry

Models are solved in 3D geometry according to two boreholes of BRIE experiment (boreholes KO0017G01 and KO0018G01). Boreholes are represented by two cylinders with different height: 3.5 m for borehole KO0017G01 and 3.1 m for KO0018G01. Diameter of both boreholes measures 30 cm.

We consider that boreholes are filled with bentonite, without any surrounding rock. Hydration through the fractures or rock-bentonite interface is described by boundary conditions. Thus it was necessary to include the lines which represents the intersections of the fracture planes with the surfaces of the borehole in the geometry (as curves on the surface of bentonite).

Fractures (two versions of distributions and number of fractures according to Task 8c and Task 8d definition are described in Figure 4-1) are included as lines which represent the intersection of the rock fractures with the borehole surface. These lines are described by dip and strike angles and vertical coordinate of the section plane of the fracture in the position of vertical axis. Intersection lines are used for prescribing of boundary conditions.

4.5 Material properties

Material parameters for determination of diffusivities were used the same as for Task 8a according to Table 3-1. Difference is in two values of rock permeabilities which were used for large-scaled 2D axisymmetric model for the determination of boundary conditions. The rock_1 permeability is 9.0×10^{-22} m^2 for the first case and the value of rock_2 permeability is 10times lower (9.0×10^{-23} m^2).

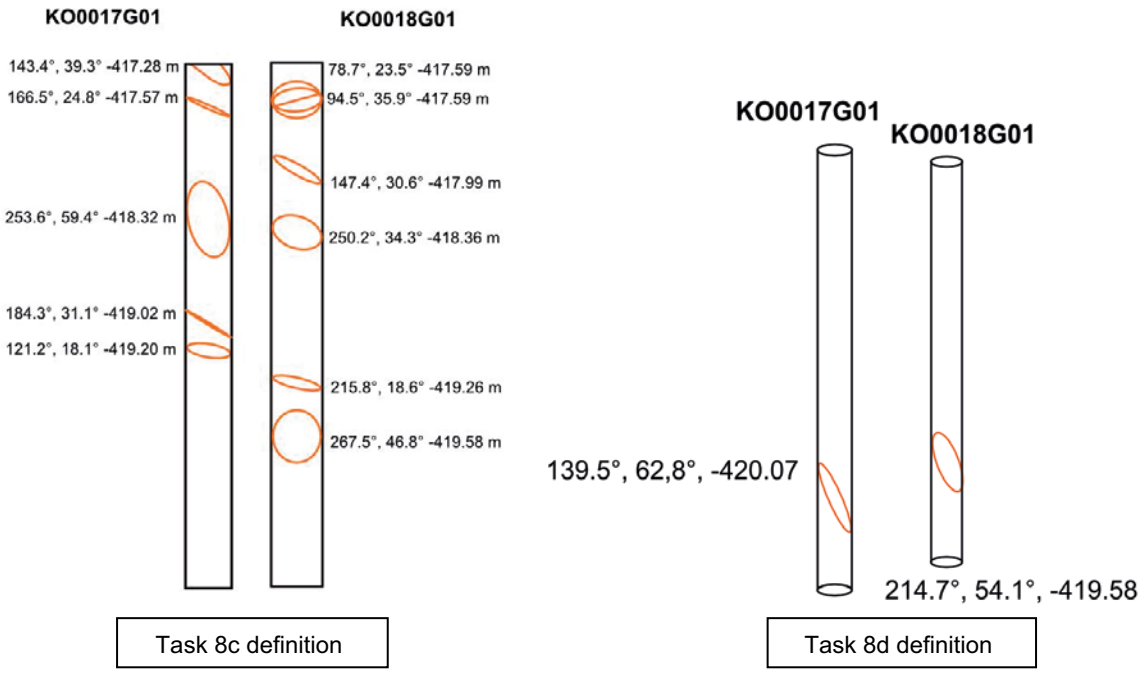

Figure 4-1. *Geometry of two model boreholes for two different model versions: LEFT: fractures according to Task 8c definition and RIGHT: fractures according to Task 8d definition, (fracture position is described by strike and dip and vertical coordinate).*

4.6 Boundary and initial conditions

Models were solved in several variants. The first version considers bentonite saturation through the fractures only, the other ones through the fracture and rock-bentonite interface. Bentonite hydration is represented by boundary conditions in our models according to Figure 4-2:

- **Hydration through the fractures:** Dirichlet's boundary condition – unlimited source of water (full saturation prescribed on lines which represents the intersection of the fracture plane and borehole surface), it is considered uniform fracture aperture.
- **Hydration through the rock-bentonite interface:** Newton's boundary condition – represented by flux dependent on degree of saturation (see 2D axisymmetric model in Chapter 3), this boundary condition is prescribed on the surface of the model (except top surface).

Dependency of the diffusive flux on the degree of saturation is determined from the rock-bentonite interface in the 2D axisymmetric model in smaller scale – we averaged the values of the fluxes in different points of the interface to get one dependency on time and then on degree of saturation. We consider the same geometry that was suggested for scoping simulations within Task 8a (Chapter 3, Figure 3-1), but the fracture is not included in the model (neglecting of the fracture influence on the flow). Decrease of the flux close to a state of full saturation expresses decreasing amount of water received to bentonite. Due to using two different values of rock permeability, two different dependencies of diffusive flux on degree of saturation were used. One of them (for rock_1 permeability) together with schematic representation of boundary conditions is referred in Figure 4-2.

Initial saturation for both boreholes was set to 36 %.

4.7 Results

We simulated bentonite hydration through the fractures and possibly through the rock-bentonite interface and then observed the evolution of saturation process. Distributions of degree of saturation for the borehole KO0017G01, without the influence of rock-bentonite interface on hydration and with it, are referred in Figure A-13 and Figure A-14.

Axial distributions of saturation for all model versions are referred in Figure A-1 to Figure A-12 (with and without rock-bentonite influence, one or several fractures, all for both boreholes – total of 12 graphs).

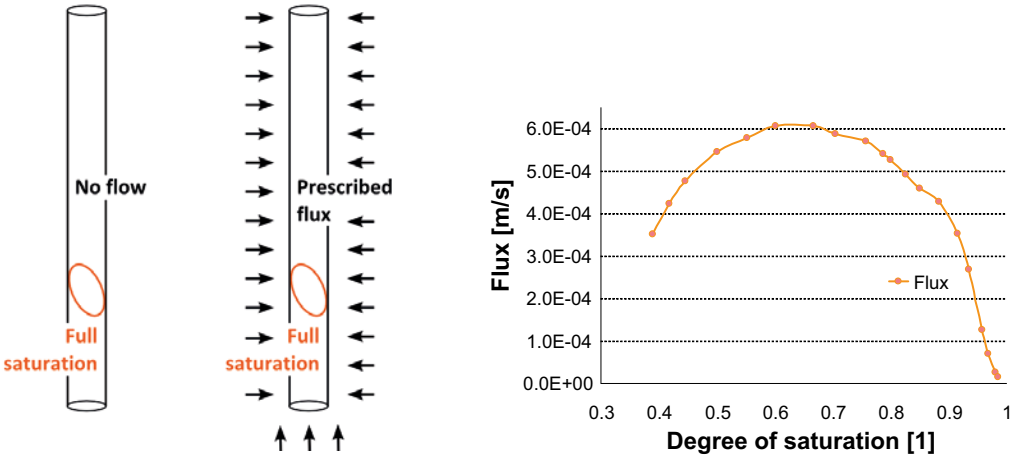

Figure 4-2. *Schematic representation of boundary conditions for the models with the influence of the fracture (and rock-bentonite hydration) and the dependency of diffusive flux on degree of saturation (according to the corresponding model considering rock_1 material) used as boundary condition representing rock-bentonite hydration.*

Times of reaching different degrees of saturation (S_l = 50 %, S_l = 75 %, S_l = 92 % and S_l = 95 %) are referred in Table 4-2 for models without rock-bentonite saturation and in Table 4-3 for models with rock-bentonite influence in comparison with results of 2D axisymmetric models. Time of reaching given degree of saturation is the time when all parts of model achieve at least this degree of saturation.

Axial profiles of saturation show that the value of degree of saturation is higher in the parts of the borehole with more fractures close to each other. Contrary for the parts of the boreholes without fractures is the process of hydration very slow (especially for models without rock-bentonite saturation). Furthermore it is also obvious that the greater dip angle indicates the longer line which specifies the intersection of fracture with the borehole surface and also the greater influence on the hydration.

4.8 Discussion

Evolution of hydration process for models with one fracture is significantly slower than for models with several fractures. It is not only a consequence of the number of fractures, but also of their positions. E.g. model variants with one fracture and more fractures: 112.8 years versus 301.1 years for 95 % saturation of the borehole KO0017G01 and 33.0 years versus 222.2 let for 95 % saturation for borehole KO0018G01.

There are also shown the consequences of differences between individual boreholes in positions of the fractures in this example – process of saturation of the borehole KO0017G01 is significantly slower and non-uniform than the process of KO0018G01 for the versions with several fractures.

Process of saturation for both borehole models with one fracture is also significantly different which depends on the position and dip and strike of the fractures (difference is almost 80 years for 95 % saturation).

Results in Figure A-1 and Figure A-2 for models with one fracture without the influence of rock-bentonite interface show similar fracture position (axial dependencies are very similar), hydration for borehole KO0017G01 is a little bit faster.

Axial distributions of degree of saturation, in Figure A-3 and Figure A-4 for models with several fractures without the influence of rock-bentonite interface, show different fractures positions. Borehole KO0017G01 does not include fractures at the bottom part of the borehole – hydration process is slower unlike the saturation of borehole KO0018G01. Local maxima in the graphs of axial distributions of degree of saturation are determined by fracture positions. In some cases two close fractures caused one wide maximum. The width of the maximum also shows the inclination of the fracture – wide maximum indicates the fracture with a high value of dip.

Table 4-3 summarizes the times of reaching 50 %, 75 %, 92 % and 95 % saturation for models with rock influence (both model versions with one or more fractures and two different rock materials denoted as rock_1 and rock_2). Results of 2D axisymmetric models are also included for comparison. We can observe significantly faster hydration unlike the models without rock influence in Table 4-2 – process of bentonite hydration is significantly influenced by the rock hydration for all solved model variants.

Times of reaching selected degrees of saturation for models with the influence of rock material called rock_1 are almost the same for all solved model variants – this also shows significant influence of rock-bentonite interface on hydration process. However more fractures indicate faster evolution of bentonite saturation.

Axial distributions of saturations in Figure A-5 to Figure A-12 also show the influence of the rock on bentonite saturation – maxima in the graphs are not so perceptible unlike models without rock-bentonite influence.

4.9 Conclusions and recommendations

We obtained times of reaching selected degrees of saturation for different model versions which depend not only on the number of the fractures but also on their positions along the borehole. Process of hydration for the boreholes with the parts without fractures is significantly slowed.

We are also able to identify the fractures (position and approximate inclination of the fracture) in axial distributions of degree of saturation – according to position and width of the local maximum in the graph.

Influence of the rock-bentonite interface on the saturation process was also simulated as boundary condition (diffusive flux) obtained from 2D axisymmetric models with two different rock permeabilities (rock materials denoted rock_1 and rock_2). These models express the case when bentonite is saturated through the fractures and through the rock together. These models show significant influence of the rock-bentonite interface on bentonite hydration for both versions of considered rock.

Table 4-2. Time necessary to reach the different degrees of saturation for 3D models with fractures and without rock-bentonite influence in comparison with time for 2D axisymmetric model without rock-bentonite influence. Time of reaching given degree of saturation is a time when all parts of model reach at least this degree of saturation.

Model	Time (S_l = 50 %) [year]	Time (S_l = 75 %) [year]	Time (S_l = 92 %) [year]	Time (S_l = 95 %) [year]
2D axisymmetric without rock-bentonite influence	22.5	50.0	85.0	97.5
3D KO0017G01 (5 fractures)	25.8	58.8	100.8	112.8
3D KO0018G01 (6 fractures)	7.5	16.9	29.2	33.0
3D KO0017G01 (1 fracture)	66.3	156.7	265.1	301.2
3D KO0018G01 (1 fracture)	50.1	115.7	194.4	222.2

Table 4-3. Time necessary to reach the different degrees of saturation for 3D models with fractures with rock-bentonite influence in comparison with time for 2D axisymmetric model with rock-bentonite influence. Two different rock materials are referred (rock_1, rock_2). Time of reaching given degree of saturation is a time when all parts of model reach at least this degree of saturation.

Model		Time (S_l = 50 %) [year]	Time (S_l = 75 %) [year]	Time (S_l = 92 %) [year]	Time (S_l = 95 %) [year]
rock_1	2D axisymmetric	0.4	0.8	1.3	1.5
Several fractures rock_1	3D KO0017G01	0.31	0.91	1.40	1.49
	3D KO0018G01	0.37	0.89	1.33	1.40
One fracture rock_1	3D KO0017G01	0.52	1.20	1.61	1.68
	3D KO0018G01	0.52	1.20	1.61	1.68
rock_2	2D axisymmetric	2.1	5.7	9.7	11.9
Several fractures rock_2	3D KO0017G01	2.8	7.4	10.4	11.0
	3D KO0018G01	2.2	5.6	7.7	8.0
One fracture rock_2	3D KO0017G01	3.52	8.5	12.0	12.6
	3D KO0018G01	3.52	8.5	12.0	12.6

5 Task 8d – comparison of modified model results with measured data (BRIE experiment)

This section builds on the previous chapter. Models of the boreholes KO0017G01 and KO0018GO1 are modified and adapted to the comparison with measured data. We consider the variant with one fracture only (see Figure 4-1 on the right) and we modified following features in the models:

- New flux boundary condition (recalculated for finer mesh of 2D axisymmetric model).
- Five different flux boundary conditions (additional values of rock permeabilities in 2D axisymmetric model) (Table 5-1).
- Different fracture aperture[3] (Table 5-2).
- Adaption of initial condition to measured data.

5.1 Model description

5.1.1 General approach

Hydration of bentonite is solved using diffusion equation described above. We consider models with simplified geometry and the influence of the fractures and rock-bentonite interface on the hydration is represented by boundary conditions – no rock is present in model geometry. The approach is the same as in Chapter 4 but we consider the variant with one fracture only.

5.1.2 Model setup

Geometry of both boreholes includes one fracture according to Figure 4-1 on the right. Material properties for bentonite remained the same as in the previous chapter. Rock influence is considered as boundary condition and different permeabilites used in 2D axisymmetric model are referred to in Table 5-1.

Fluxes used within boundary condition are determined from the 2D axisymmetric model in large scale. We assume fluxes dependent on degree of saturation – they are estimated from the gradient of degree of saturation at the rock-bentonite interface and diffusivity of bentonite.

Table 5-1. Material properties for rock and bentonite for comparison of model results with measured data, rock material was used for boundary condition estimation in 2D axisymmetric model.

	P_0 [MPa]	λ [1]	k [m^2]	n [1]	μ [Pa × s]
Bentonite	9.23	0.3	9.5×10^{-21}	0.438	10^{-3}
Rock 1	1.74	0.6	9.0×10^{-22}	0.003	10^{-3}
Rock 2	1.74	0.6	9.0×10^{-23}	0.003	10^{-3}
Rock 3	1.74	0.6	1.5×10^{-22}	0.003	10^{-3}
Rock 4	1.74	0.6	7.5×10^{-23}	0.003	10^{-3}
Rock 5	1.74	0.6	9.375×10^{-24}	0.003	10^{-3}

Models were solved with above mentioned boundary condition (representing hydration through the fracture and rock-bentonite interface). Flux boundary condition was considered in five variants (“Rock 1” to “Rock 5”, Figure 5-1) to capture different permeabilities of surrounding rock.

[3] It was changed rock permeability (represented by boundary condition) and the aperture of the fracture. There is no material parameter assigned to the fracture which could express the fracture transmissivity, (the only input is diffusivity of the bentonite).

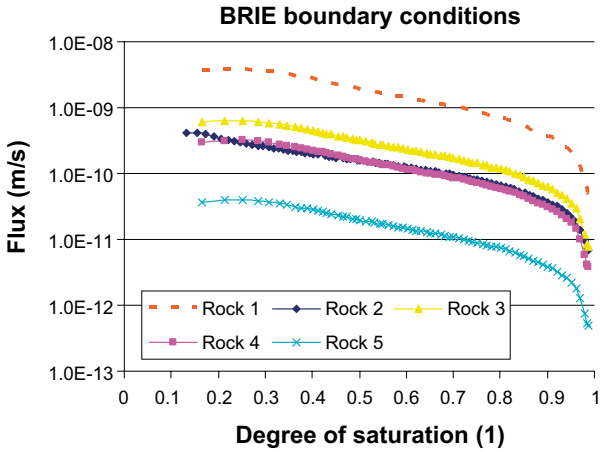

Figure 5-1. *Boundary condition which represents flux through the rock-bentonite interface (five different values of rock permeability– material "Rock 1" to "Rock 5").*

Additionally it was tested several different fracture "apertures" for both boreholes together with boundary condition according to "Rock 5" on the surface of the borehole. Within this case fracture is represented by a thin band with the same boundary condition (full saturation) – the same as for line fracture. Unfortunately it is not possible to determine the fracture transmissivity due to model conception and fracture setup[4]. Solved model variants according to boundary condition are referred in to Table 5-2.

Initial bentonite saturation is set to 42 % (because of better accordance with measured data unlike the recommended value 36 %).

Table 5-2. Tested model variants (combinations of different boundary conditions and eventually fracture aperture) for comparison of model results with measured data.

Model version	Boundary condition	Fracture	
		KO0017G01	KO0018G01
1	Rock 1	Fracture as a line	Fracture as a line
2	Rock 2		
3	Rock 3		
4	Rock 4		
5	Rock 5		
6	Rock 5	2.3 cm	2.9 cm
7	Rock 5	4.6 cm	1.2 cm

5.2 Model results for borehole KO0017G01

It was solved several model variants according to Table 5-2 with five different flux boundary conditions prescribed on the surface of the borehole and additionally two different fracture apertures (2.3 cm and 4.6 cm) for borehole KO0017G01. This unrealistic aperture does not correspond to the real fracture aperture. It is just geometric parameter through which we are partly able to increase the water supply to the bentonite (through the fracture as boundary condition).

[4] Transmissivity of the fracture is not possible to determine because it is represented by the boundary condition. Fracture is not a part of the model; it is only a line (or part of the surface) which serves for prescription of b.c. and it cannot have material properties.

Times of reaching different degrees of saturation (time when all parts of model reach at least this degree of saturation) for all models are referred in Table 5-3. Times are very different because of various boundary conditions (the model without rock influence is also shown for comparison and it is slightly different from the values in Table 5-2 due to different initial conditions[5] and simulation time step). The progress of hydration is mainly influenced by uniform inflow through the rock-bentonite interface (on the other hand hydration through the fracture causes significant local inhomogeneity in the fracture vicinity). In the case of the model variants with "Rock 5" boundary condition (the lowest permeability of the rock in 2D axisymmetric model) was reached 95 % saturation in 30 years, in the cases with higher values of rock permeability in several years. Rock 1 seems to be less relevant in our models due to the more significant influence (stronger than fracture influence) of this derived boundary condition on the bentonite saturation (in comparison with measured data). It is connected with unclear estimation of flux boundary conditions which express the rock influence on bentonite saturation (Section 3.5).

Model results were compared with measured data (degree of saturation in the cross-sections of the boreholes and profiles of relative humidity and degree of saturation in sensor positions). Measured distributions of relative humidity were converted to degree of saturation using Kelvin law and retention curve in our case. Visual comparison is quite problematic but distribution of degree of saturation in cross-sections qualitatively corresponds to measured data (Figure A-19, Figure A-20 and Figure A-21).

Best match of RH distributions in sensor positions was reached for model variant 6 and 7 with 2.3 and 4.6 cm fracture aperture (all profiles together in Figure 5-3 and individually in Figure A-15 and Figure A-16). For model variant 6 is reached better accordance in the sensor position W1, for variant 7 in the sensor position W3, distribution in other sensors positions shows similar correspondence with measured data. This implies more conductive zone near the W3 position (which is consistent with the measured data).

The hydration is a little bit overestimated in the fracture vicinity in both variant. The rest of the model reached slightly lower values of degree of saturation according to Figure A-20 and Figure A-21 (comparison of measured data with model results in cross-sections) – the lowest value of the degree of saturation is 44 % in models with "Rock 5" boundary condition.

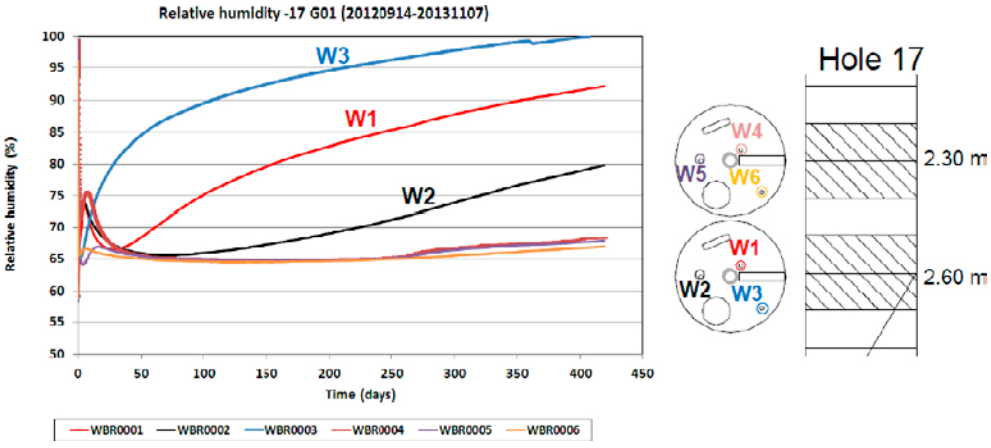

Figure 5-2. *Measured profiles of relative humidity in the borehole KO0017G01 with displayed positions of sensors, adapted from Fransson et al. (2017).*

[5] Initial saturation in model was changed due to false initial assumption – different initial degree of saturation in comparison with real measured initial RH (converted to degree of saturation).

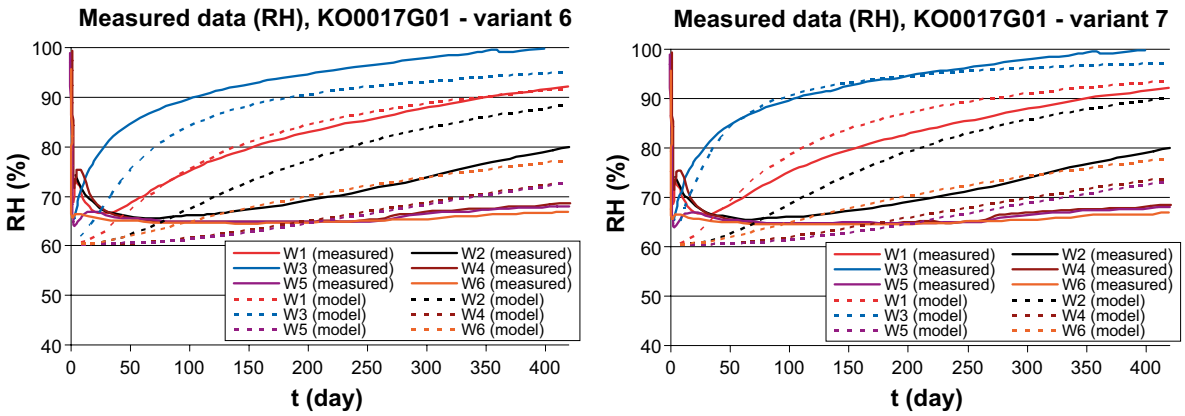

Figure 5-3. *Comparison of measured data with model results (relative humidity in the borehole KO0017G01 for variant 6 and 7).*

Table 5-3. Times necessary to reach different degrees of saturation for different model variants. Time of reaching given degree of saturation is a time when all model parts reach at least this degree of saturation.

Borehole	Model variant	Time (S_l = 50 %) (year)	Time (S_l = 75 %) (year)	Time (S_l = 92 %) (year)	Time (S_l = 95 %) (year)
KO0017G01	Without rock influence	50.7	152.2	263.8	304.4
	1	0.18	0.36	0.42	0.43
	2	0.6	2.0	3.0	3.1
	3	0.5	1.5	2.1	2.2
	4	0.8	2.8	4.1	4.3
	5	4.9	20.9	30.7	32.1
	6	4.9	20.9	30.7	32.1
	7	4.9	20.9	30.7	32.1
	8	4.9	20.9	30.7	32.1
KO0018G01	Without rock influence	38.1	107.8	196.6	222.0
	1	0.17	0.36	0.42	0.43
	2	0.6	2.0	3.0	3.1
	3	0.2	1.5	2.1	2.2
	4	0.9	2.8	4.1	4.3
	5	4.9	20.2	29.3	30.7
	6	4.9	20.2	29.3	30.7
	7	4.9	20.2	29.3	30.7

5.3 Model results for borehole KO0018G01

It was solved several model variants according to Table 5-2 with five different flux boundary conditions prescribed on the surface of the borehole and additionally two different fracture apertures (2.9 cm and 1.2 cm) for borehole KO0018G01.

Times of reaching different degrees of saturation are similar as in the case of borehole KO0017G01 (about 30 years for 95 % saturation within “Rock 5” boundary condition and several years for other relevant variants) – the times for the borehole without fractures is slightly different from the times in Table 5-2 because different initial condition and simulation time step.

Distributions of relative humidity (or degree of saturation) were also compared with measured data in sensor positions. The best correspondence has been noticed for the version 6 with "Rock 5" boundary condition and 1.2 cm fracture aperture. Nevertheless, the correspondence was worse than in the case of borehole KO0017G01. Proper agreement was achieved in sensor positions W9 and W11 – which refers to different and identified and real fracture position.

Corresponding of degree of saturation in cross-sections with measured data (Figure A-22, Figure A-23) is worse than for the borehole KO0017G01. Measured data indicates other positions of water inflow which are not captured in our models (which also corresponds to comparison of time distribution of degree of saturation and relative humidity in sensor positions).

Unlike the borehole KO0017G01 hydration near the fracture is not overestimated (sensor positions W7, W8 and W9). Model reaches lower degree of saturation than measured data in sensor positions which are more distant from the fracture (W10, W11 and W12). Distributions of degree of saturation and relative humidity in comparison with measured data are described in Figure 5-5 and also in separately in Figure A-17.

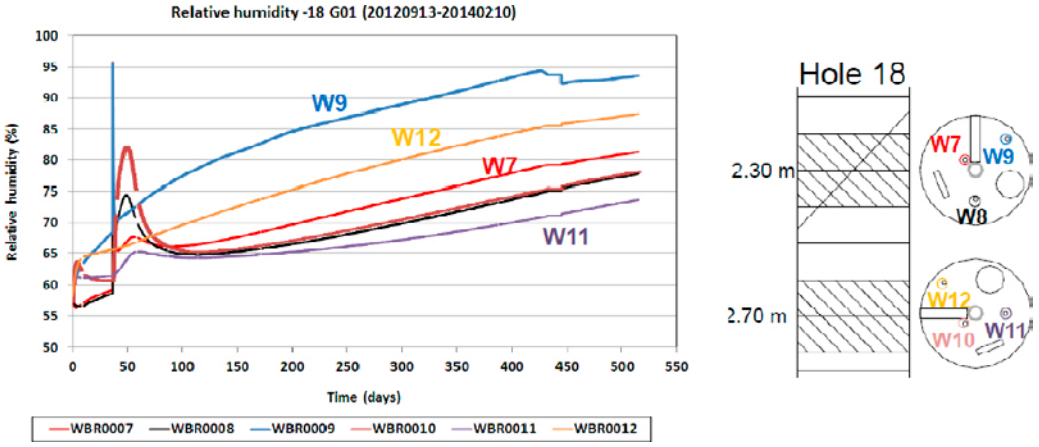

Figure 5-4. *Measured profiles of relative humidity in the borehole KO0018G01 with displayed positions of sensors, adapted from Fransson et al. (2017).*

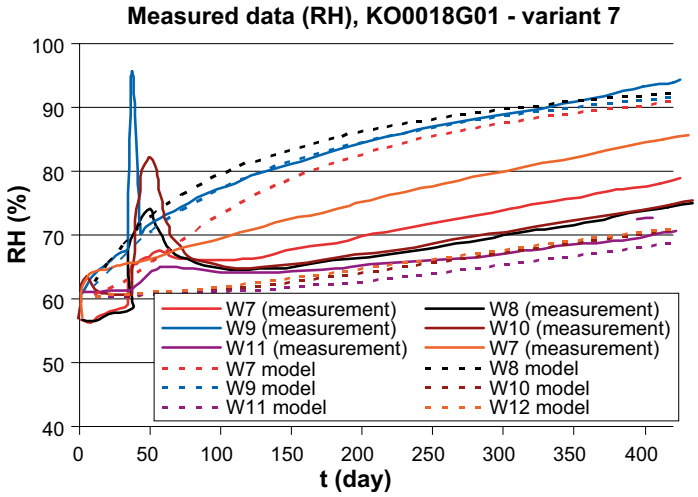

Figure 5-5. *Comparison of measured data with model results (relative humidity in the borehole KO0018G01 for variant 7).*

5.4 Conclusions

Based on results of our models we are able to represent hydration of bentonite using simplified models without rock in small scale. Limitations of our models result from used model conception (diffusion equation with nonlinear diffusivity and degree of saturation as a dependent variable). The influence of the fractures and rock-bentonite interface on bentonite saturation is represented by boundary conditions which are estimated from 2D axisymmetric models with rock in larger scale.

The process of hydration is mainly influenced by the positions and of water inflows (fractures, conductive zones), amount of free water and material parameters of bentonite and rock. The fracture positions are considered as a main uncertainty in our models. According to our results fracture position corresponds with assumed position in borehole KO0017G01. The results for borehole KO0018G01 shows certain shift of the fracture position and probably the other source of water besides the expected.

Figure 5-3 and Figure 5-5 show dependencies of measured relative humidity on time in comparison with model data (degree of saturation converted to relative humidity) for both boreholes. Based on these graphs it seems that saturation is very slow in the parts distant from the fractures (and we had to use boundary condition based on very low value of rock permeability). The reason is not clear but in comparison with results of other modelling groups it is obvious that the value of rock permeability is not realistic.

The influence of the fractures on bentonite saturation is possible to express by boundary condition (Dirichlet's b.c. – unlimited source of water) but it is quite problematic to estimate fracture transmissivity. Because the only parameter, which we are able to change, is fracture aperture. (Hydraulic conductivity of fracture do not enter to the model because fracture has no material – it is just boundary condition).

6 Summary and conclusions

6.1 Summary

Initial calculations were performed for axisymmetric model in Flow123D as a sensitivity study for flow in saturated conditions.

Then we solved bentonite hydration using diffusion equation with nonlinear diffusivity. 2D axisymmetric model solved as problem of flow in partly saturated conditions using was used for testing and comparison with some scoping calculations in Code_Bright.

Further hydration of bentonite in 3D models of boreholes KO0017G01 and KO0018G01 was simulated in a simple geometry. Surrounding rock and fractures were not physically included in the model. We consider their influence via boundary conditions. We solved several variants of the models with one or several fractures (according to Task 8d or Task 8c definition) and also without or with the influence of surrounding rock. These models were then modified and compared with measured data in the boreholes KO0017G01 and KO0018G01.

6.2 Conclusions

Initial calculations in Chapter 3 and 2D axisymmetric model were solved as initial calculations for becoming familiar with the modelling of bentonite hydration.

Different situations are described in the sensitivity study for the inflow into the fracture for saturated conditions. And thus we obtain the insight into the problem.

In Task 8a we compared results of the models solved in Ansys (diffusion equation) with scoping calculations in Code_Bright (Richards' equation) with problems in the expression of the rock influence on bentonite saturation. Good correspondence was reached after the modification of the material parameters (original parameters according to Vidstrand et al. (2017) – specifically increase the values of bentonite and rock permeability. Unfortunately this uncertainty and difference has not been explained yet (see Section 3.5).

For the Task 8d calculations we obtained times of reaching selected degrees of saturation for different model versions which depend not only on the number of the fractures but also on their positions along the borehole. Process of hydration for the boreholes with the parts without fractures is significantly slowed. We are also able to identify the fractures (position and approximate inclination of the fracture) in axial distributions of degree of saturation – according to position and width of the local maximum in the graph.

Influence of the rock-bentonite interface on the saturation process was also simulated as boundary condition (diffusive flux) obtained from 2D axisymmetric models with two different rock permeabilities (five different variant). These models show significant influence of the rock-bentonite interface on bentonite hydration.

Models of Task 8d which were modified (in rock material parameters through boundary condition, fracture aperture and initial condition) and compared with measured data. We obtain satisfactory qualitative agreement for some model variants within borehole KO0017G01. But the correspondence in qualitative terms is not so good – it is very problematic to set the right combination of rock permeability and fracture transmissivity (limited possibility to modify fracture aperture). Results for borehole KO0018G01 match in selected positions only and total correspondence is worse – distributions of degree of saturation indicate additional inflow positions.

6.3 Open issues

Uncertainty in our models could be reduced by following additional features and data (if it is possible to obtain it):

- More precise fracture position should help for definition of boundary conditions in our models to improve the positions of inflow to bentonite and way of bentonite hydration.
- Data obtained from laboratory experiment with water saturation imitating a fracture (inhomogeneous water inflow with controlled flow rate or pressure).
- Complete the numerical model with the features of the "reified model" (Richards' equation with added water transport through the water vapour) and compare the differences between results for both concepts.

7 Additional information according to the questionnaire

7.1 True system, reified model, and actual model

7.1.1 True system

Current system understanding and concept of the processes in bentonite and in the rock and other important issues are described in this part.

We consider water flow in partly saturated conditions (in both bentonite and granite) – water distribution in bentonite is controlled by temperature (temperature dependence in general – on the other hand BRIE experiment is considered at a constant temperature). Behaviour of the system can be described by multiphase flow with the influence of the pressure-saturation relation (retention curve), hydraulic conductivity of the medium, diffusion of water vapour, storativity, etc.

Water flow through the fractures dominates over the flow through the rock matrix and fractures positions have significant influence on hydration of bentonite in the borehole.

A possible gap between rock and bentonite blocks (or other non-ideal contact) is present in real configuration but this feature is usually neglected in the models.

Distribution of water pressure in the rock is influenced by far-field effects (other underground constructions, tunnels etc). The other features and properties of the system are in accordance with Task 8 definition.

7.1.2 Reified model

Process of bentonite saturation is described by coupled system of THM equations (for multiphase flow in connection with the heat transfer equations and equations for mechanical behaviour). While the diffusion of water vapour, dependence of the material properties on temperature and contact behaviour between rock and bentonite are considered.

It should be known detailed description of surrounding rock and all discontinuities and conductive zones (including all man-made structures and effects) and also detailed description of considered materials (bentonite and granite with all material properties). It should be also used an accurate representation of imperfect contact.

7.1.3 Actual model

Bentonite hydration is described using diffusion equation with nonlinear diffusivity dependent on degree of saturation (transformation of Richards' equation according to Börgesson 1985).

- No rock is considered in the models.
- Bentonite hydration is represented by boundary conditions (hydration through the fractures is represented by full saturation b.c., hydration through the rock is represented by flux b.c. dependent on degree of saturation).
- Information about water flow across rock-bentonite interface is derived from the axisymmetric model in smaller scale (supporting model below).
- Initial bentonite saturation 36 %.
- Different fracture aperture (transmissivity) is not considered.
- Given constitutive relations (based on laboratory tests) without changes.

- Supporting model features:
  - 2D axisymmetric models with rock and fracture (represented by permeable rock material),
  - van Genuchten retention curve for bentonite, square law retention curve for rock and fracture for an estimation of boundary conditions for models in smaller scale.

More detailed information is given in Chapter 3 and 4.

7.1.4 Alternative model

Another alternative concept that could be used for modelling of bentonite hydration is model that combines larger-scale approach (which includes bentonite and rock in the geometry) and smaller scale approach (bentonite-only model).

The other possible conception is commonly considered multiphase models.

7.2 Input and prior uncertainties

7.2.1 Prior uncertainties

The most important uncertainties in our models are connected with information about positions of inflow into the borehole (sources of water for bentonite hydration) – the positions of boundary conditions which have significant influence on the way and rate of bentonite saturation.

Other relevant uncertainties are:

- Pressure in the fracture is depending on time,
- No information about uniformity of inflow/transmissivity in the fracture plane around the borehole circumference (fractures in our models have uniform transmissivity – aperture that is not possible to change and control the water inflow through the fracture),
- Uncertainty about Richards' equation if it has a dominant influence in water transport to bentonite (other mechanisms of water transport to bentonite are not included)

7.3 Sensitivities

7.3.1 Impact on understanding

- Our models describe the process of bentonite saturation in more realistic way than uniform flow and estimate the influence of the matrix water on hydration.
- Solved examples should show that simplified models could bring relatively corresponding results. And also provide any recommendations how to simplify the models which bring as far as possible relevant results.
- Balancing the suction of bentonite and the rock/fracture water availability not captured.

7.3.2 Impact on predictions

The results should influence the prediction of:

- Progress of saturation of bentonite over time (due to the fracture positions and the hydraulic conductivity of the rock and fracture transmissivity).
- Degree of homogeneity of the saturation process (due to the influence of fractures or surrounding rock).
- Mechanical behaviour (indirectly through saturation process).

7.4 Input and prior uncertainties

7.4.1 Ranking of features

Ranking of features according to their potential impact on overall system understanding and numerical model predictions:

1. Fracture positions.
2. Fracture transmissivity.
3. Simplification of the gap between bentonite and rock.
4. Bentonite retention curve.
5. Equation of water transport in bentonite.

7.4.2 Weighting of features

It is not possible to assign weight to the ranked model features to reflect the order of magnitude of the expected impact.

7.5 Prediction uncertainty

7.5.1 Uncertainty in understanding

The degree of confidence about the overall system: medium.

Quite sure with the process of water transport in bentonite, unsure with the mechanism controlling the water availability, what is the critical rock/fracture parameter (conceptual uncertainties correspond to uncertainties of predictions with Richards' equation, neglecting the influence of water vapour is not so important at constant temperature conditions).

7.5.2 Uncertainty in predictions

The degree of confidence in our model predictions given conceptual uncertainties and their impact on these predictions: medium/small.

Our model conception is unable to identify accurately the amount of water available to bentonite. The other uncertainty is in the rate of saturation in time and how the closing a gap and in the ratio between fracture contact and matrix contact.

7.6 Calibration and prediction

7.6.1 Data uncertainty

Experimental conditions within **Water Uptake Test (brief description in Appendix A.1)** fit the model assumptions, we do not find (critical) uncertainties in the process, but some uncertainty could be e.g. in material or inflow inhomogeneity.

The fine spatial resolution of **BRIE** is valuable, but even the visual comparison of rock phenomena "inputs" (fracture positions, pressure tests, water inflow) and bentonite hydration "outputs" (degree of saturation distributions) show inconsistencies suspecting processes which cannot be captured by model data – defined positions of fractures do not fully correspond to degree of saturation distribution for borehole KO0018G01, better correspondence is reached for KO0017G01).

7.6.2 Expected residuals

Our models can reproduce (or predict):

- General trend.
- Order-of-magnitude behaviour.
- Spatial distribution of general trends.

7.6.3 Prediction

Our models predict behaviour of the **WUT** models quite well – results correspond to measured data similarly as Code_Bright results presented in the document related to WUT modelling. This correspondence is achieved due to known position of water supply (and its rate).

Results of the **BRIE** models qualitatively correspond with the distribution of measured hydration. The influence of the fracture on hydration is **underestimated** (the fracture transmissivity is not possible to parameterize in model) and the influence of the rock matrix is **overestimated** (possible change of the rock permeability through the flux boundary condition).

The results for BRIE models had to be calibrated (the change boundary condition through the rock permeability of 2D axisymmetric model in larger scale).

7.6.4 Calibration

Results of **WUT** models reproduce the behaviour of experiment quite well and no calibration has been performed.

Calibration of permeability of the rock matrix on saturation results had to be performed in the case of BRIE models. The influence of the rock matrix on hydration was overestimated, that decrease of rock permeability within flux boundary condition in 2D axisymmetric model causes more appropriate hydration rate.

Results of some model variants corresponds with measured data (in the quantitative and qualitative aspect) – for borehole KO0017G01, results of borehole KO0018G01 not fully agree with measured data due to in-precise fracture (conductive zone) position.

7.7 Specific predictions

7.7.1 Predictions

We have no predictions for inflow into the open holes KO0017G01 and KO0018G01 because no open-hole calculations have been performed.

Information about hydration process in both boreholes filled with bentonite is presented in Table 7-1 for chosen variant. Referred saturation is the lowest value of degree of saturation in the model in the end of simulation (419 days for model of the KO0017G01 and 518 days for model of the KO0018G01). Table 7-1 also shows the time of bentonite resaturation to 95 %. Detailed information about other variants is referred in Table 4-3 and Table 5-3.

Table 7-1 Material properties for rock and bentonite.

	KO0017G01	KO0018G01
Degree of saturation (in the end of simulation)	54 %	58 %
Time of bentonite resaturation to 95 %	3.7 years	3.7 years

7.7.2 Uncertainty

Different values of permeability of the host rock (range two orders of magnitude) used in the models in larger scale – for definition of boundary conditions. The higher rock permeability ($k = 9 \times 10^{-22}$ m^2) causes dominant effect of the rock on bentonite hydration, for lower rock permeability ($k = 9 \times 10^{-24}$ m^2) fracture has significant influence on bentonite hydration. Other uncertainties are not considered in our models.

7.7.3 Conceptual uncertainty

We used different definitions of retention curve and relative permeability for bentonite in WUT models, with recommended relations and recommended parameter values.

Retention curve	**Relative permeability relation**
van Genuchten ($P_0 = 10$ MPa, $\lambda = 0.28$)	$K_r = S_l^3$
square law ($P_0 = 19.3$ MPa)	$K_r = S_l^4$

No other evaluation of uncertainties has been done.

7.8 General assessment

7.8.1 Understanding

The main improvement in system understanding gained by performing Task 8 is in following features:

- The rock-controlled bentonite hydration is realistic phenomenon and an important issue in engineered barrier system construction.
- Our models show that using an alternative conception (diffusion equation with nonlinear diffusivity) with some simplifications brings quite good results but it is necessary to carefully use inputs to the models and check input data.
- The particular data of rock matrix are not enough to predict full 3D bentonite saturation.
- It was confirmed that for correct representation of overall hydration rate it is necessary to represent correctly and precisely the properties of rock matrix (material properties, retention curve, positions of more permeable zones) and fracture (position, transmissivity).

7.8.2 Change in uncertainty

After new data were incorporate into the model we included more accurate positions of fractures and hydraulic properties of the host rock to allow more precise description of bentonite hydration process (fracture positions may not correspond with inflow position). The next issue is a relation of a-priori matrix permeability and its value in calibration.

7.8.3 Conceptual uncertainty

The main features in the models are captured quite well (specifically: general process of water flow and its distribution). But there are several influences that are not clear from the data:

- The cases when rock water and bentonite hydration positions do not fit (especially fracture position for borehole KO0018G01).
- Water transport processes along the bentonite/rock interface – the relation between the gap and water inflow and possible flowing down the borehole wall.

7.8.4 Model uncertainty

Describe the degree to which the current numerical model is believed to represent the behaviour of the true system.

Due to simplifications in our models is the representation of reality limited but with relatively good description of the trends in the process (hydration from positions of given water inflow). The predicted overall rate of hydration is only rough estimate (there in no direct link to the hydraulic properties and changing pressure).

7.8.5 Key uncertainty

The main aspects of our model which are the main source of insufficient system understanding and predictive uncertainty are:

- Variable transmissivity in a fracture plane which is not captured in our models.
- Rock matrix permeability value – we are not sure why our model overestimates the inflow through the rock matrix.
- Pressure evolution in rock as the consequence of bentonite saturation which is also not included in our models.

7.8.6 Research plan

Mentioned uncertainty in our models could be reduced by following additional features and data (if it is possible to obtain it):

- More precise fracture position should help for definition of boundary conditions in our models to improve the positions of inflow to bentonite and way of bentonite hydration.
- Data obtained from laboratory experiment with water saturation imitating a fracture (inhomogeneous water inflow with controlled flow rate or pressure).
- Complete the numerical model with the features of the “reified model” (Richards’ equation with added water transport through the water vapour) and compare the differences between results for both concepts.

References

SKB's (Svensk Kärnbränslehantering AB) publications can be found at www.skb.com/publications.

ANSYS, 2010. ANSYS Academic Research, Help System. version 13.0. Canonsburg, PA: Ansys, Inc.

Börgesson L, 1985. Water flow and swelling pressure in non-saturated bentonite-based clay barriers. Engineering Geology 21, 229–237.

Fransson Å, Åkesson M, Andersson L, 2017. Bentonite Rock Interaction Experiment. Characterisation of rock and installation, hydration and dismantling of bentonite parcels. SKB R-14-11, Svensk Kärnbränslehantering AB.

Vidstrand P, Åkesson M, Fransson Å, Stigsson M, 2017. SKB Task Forces EBS and GWFTS. Modelling the interaction between engineered and natural barriers. A compilation of Task 8 descriptions. SKB P-16-05, Svensk Kärnbränslehantering AB.

Appendix 1

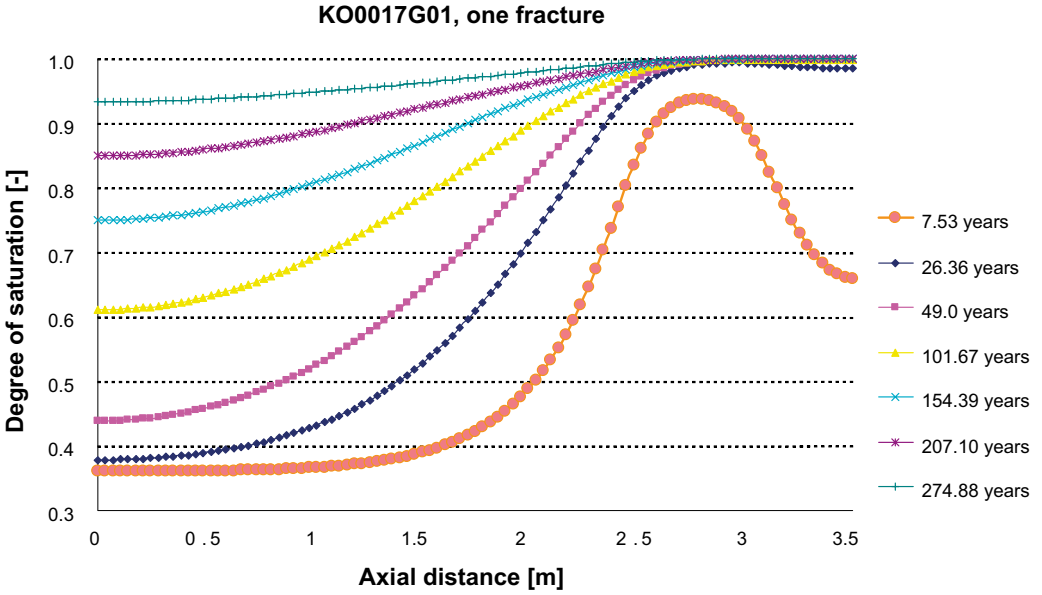

Figure A-1. *Axial distributions of degree of saturation for the borehole KO0017G01 over time with one fracture (according to Task 8d definition) without the rock-bentonite influence.*

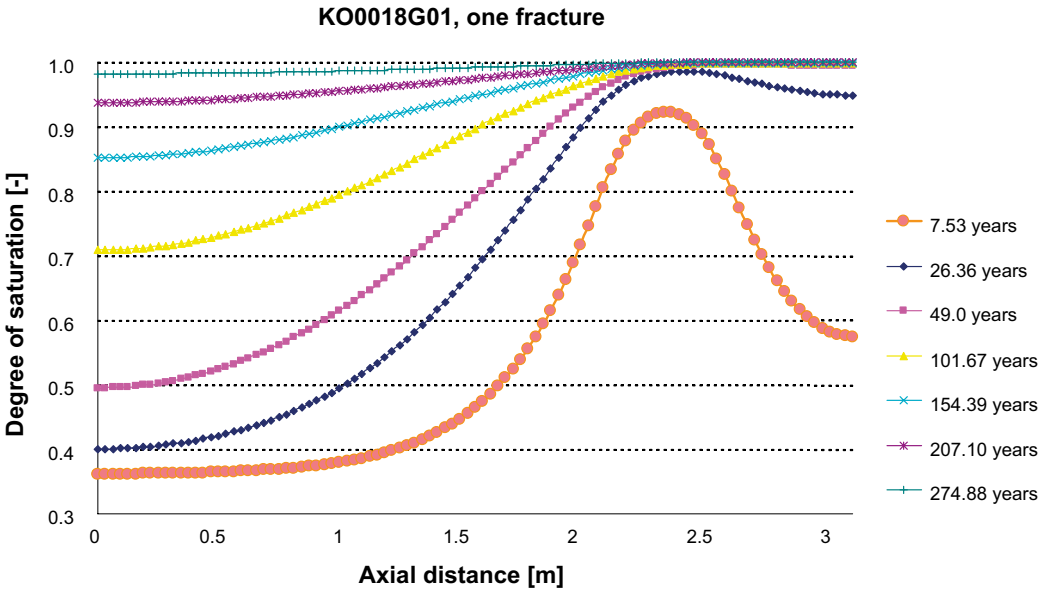

Figure A-2. *Axial distributions of degree of saturation for the borehole KO0018G01 over time with one fracture (according to Task 8d definition) without the rock-bentonite influence.*

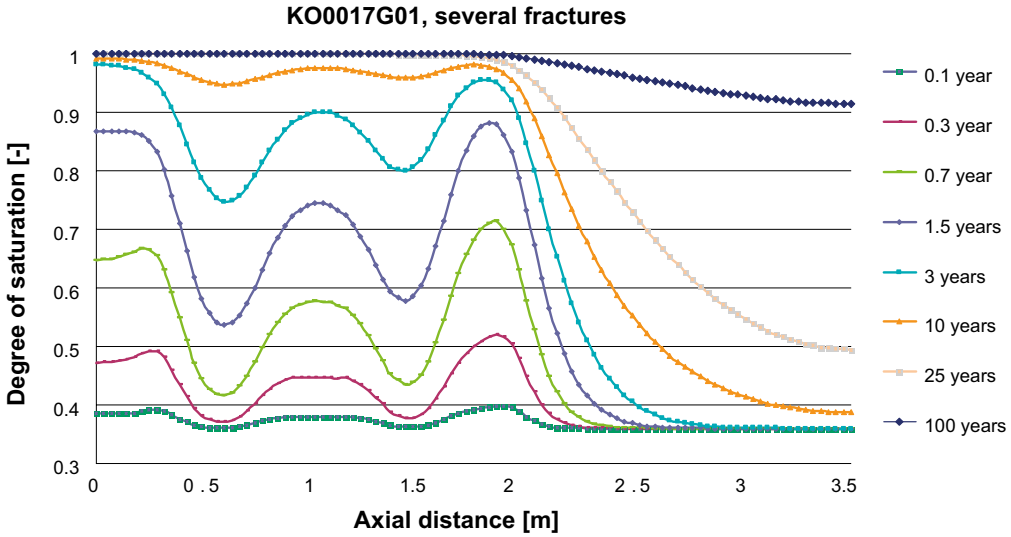

Figure A-3. *Axial distributions of degree of saturation for the borehole KO0017G01 over time with several fractures (according to Task 8c definition) without the rock-bentonite influence.*

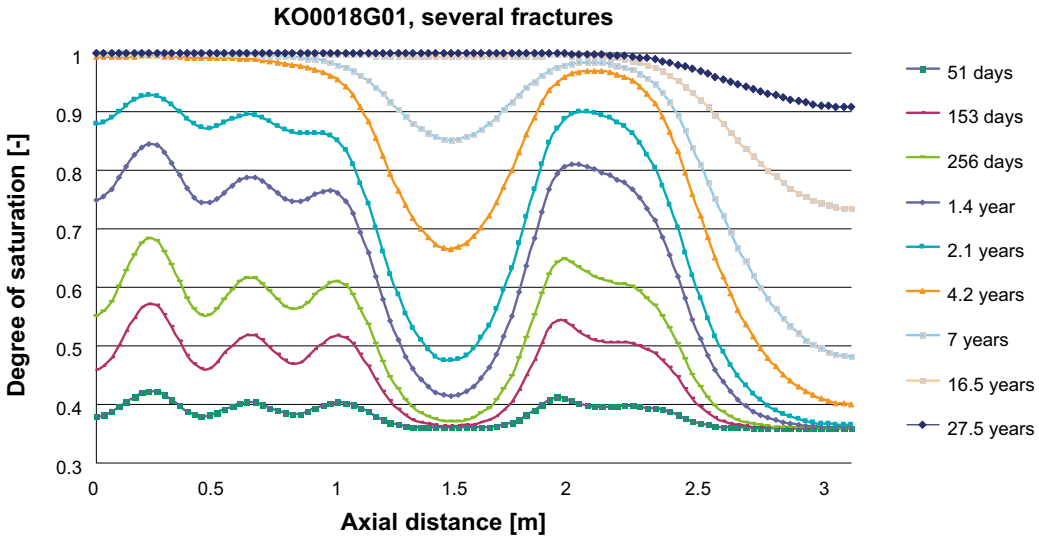

Figure A-4. *Axial distributions of degree of saturation for the borehole KO0018G01 over time with several fractures (according to Task 8c definition) without the rock-bentonite influence.*

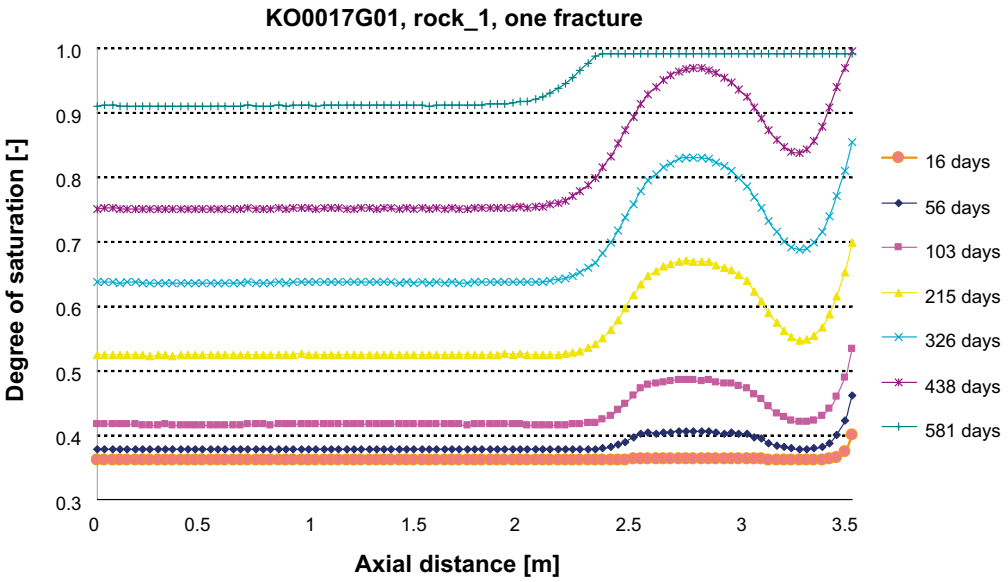

Figure A-5. *Axial distributions of degree of saturation for the borehole KO0017G01 over time with one fracture (according to Task 8d definition) with the rock-bentonite influence (rock_1 material).*

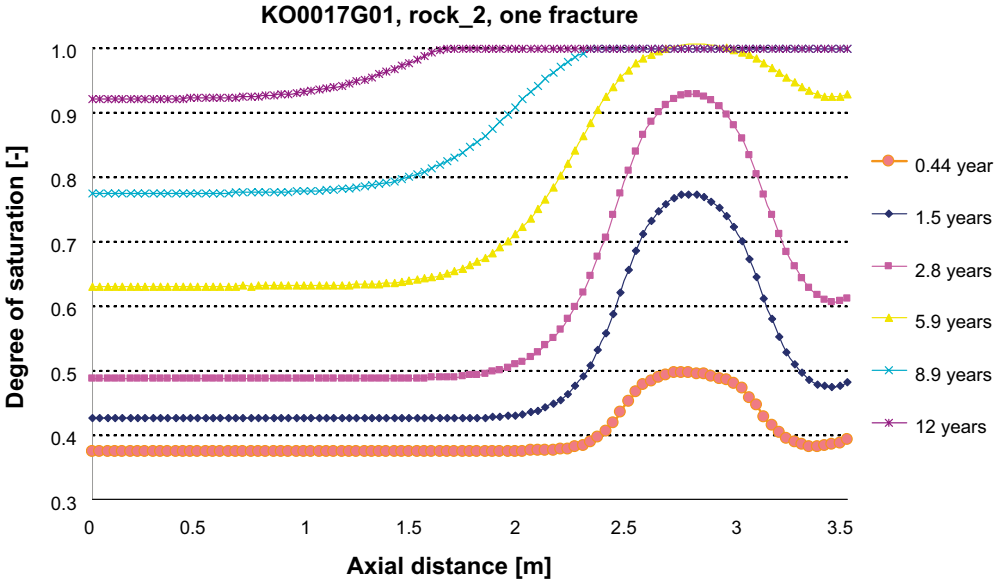

Figure A-6. *Axial distributions of degree of saturation for the borehole KO0017G01 over time with one fracture (according to Task 8d definition) with the rock-bentonite influence (rock_2 material).*

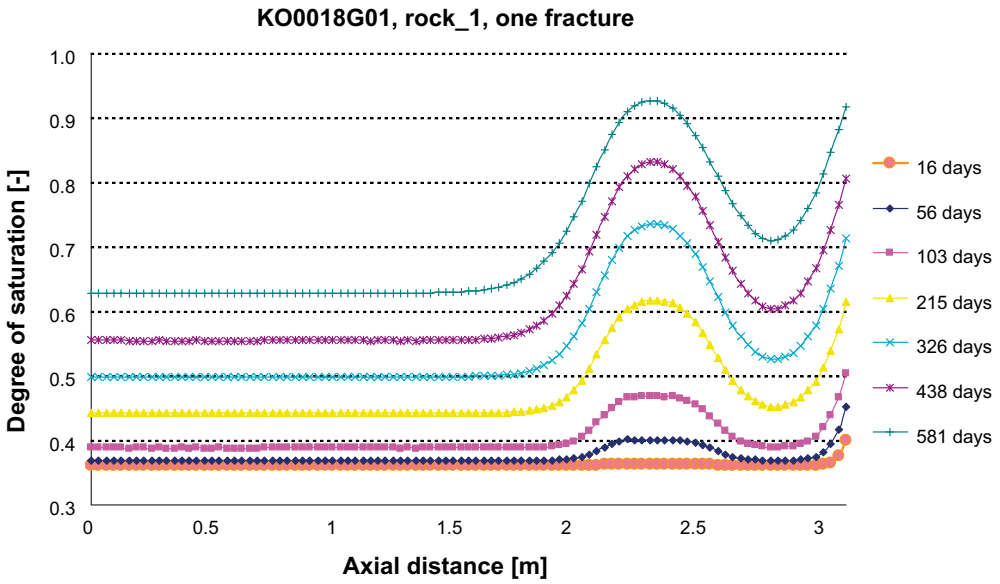

Figure A-7. *Axial distributions of degree of saturation for the borehole KO0018G01 over time with one fracture (according to Task 8d definition) with the rock-bentonite influence (rock_1 material).*

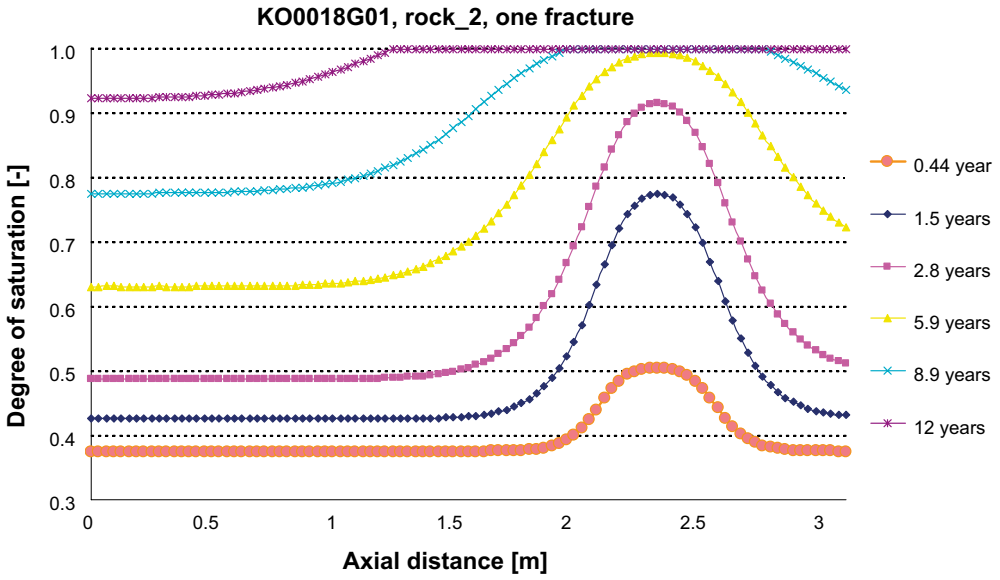

Figure A-8. *Axial distributions of degree of saturation for the borehole KO0018G01 over time with one fracture (according to Task 8d definition) with the rock-bentonite influence (rock_2 material).*

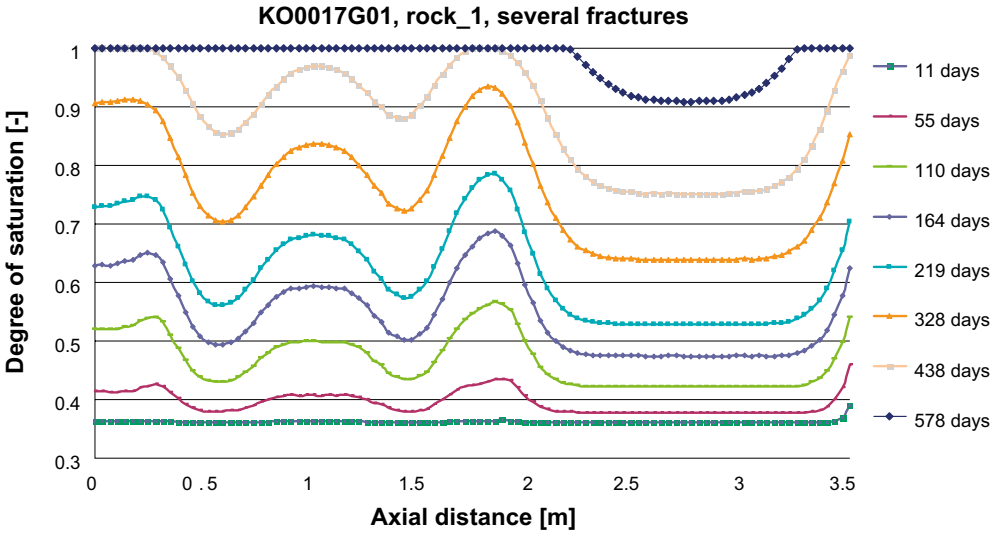

Figure A-9. *Axial distributions of degree of saturation for the borehole KO0017G01 over time with several fractures (according to Task 8c definition) with the rock-bentonite influence (rock_1 material).*

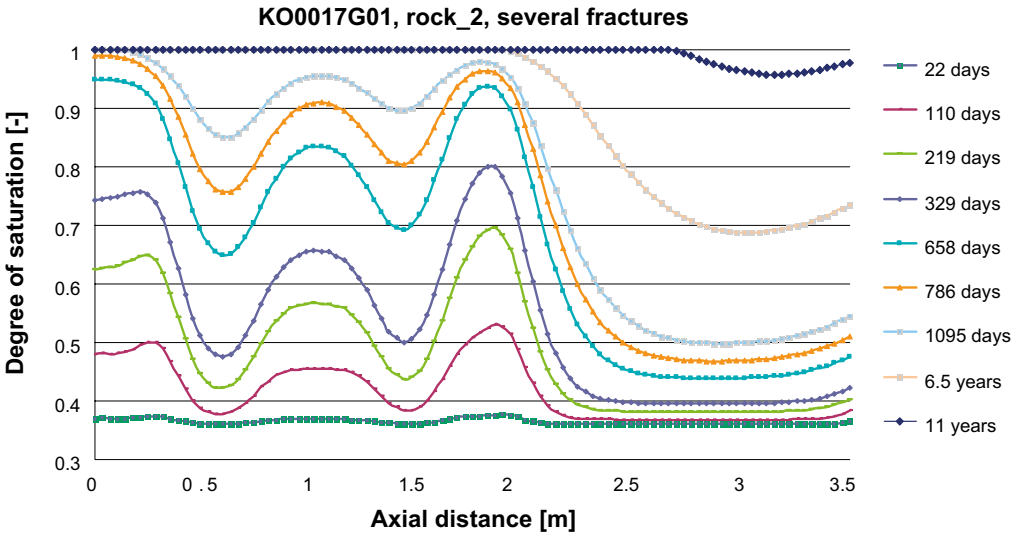

Figure A-10. *Axial distributions of degree of saturation for the borehole KO0017G01 over time with several fractures (according to Task 8c definition) with the rock-bentonite influence (rock_2 material).*

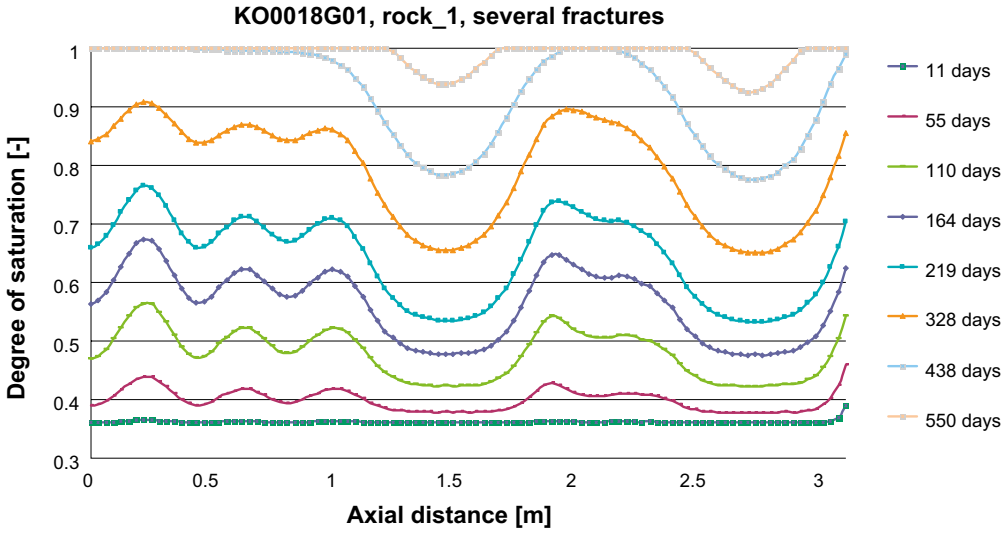

Figure A-11. *Axial distributions of degree of saturation for the borehole KO0018G01 over time with several fractures (according to Task 8c definition) with the rock-bentonite influence (rock_1 material).*

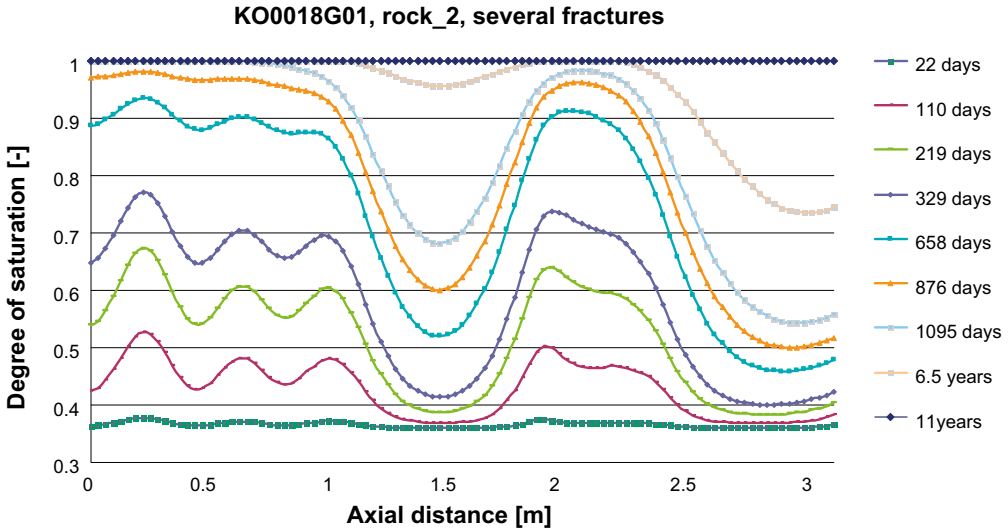

Figure A-12. *Axial distributions of degree of saturation for the borehole KO0018G01 over time with several fractures (according to Task 8c definition) with the rock-bentonite influence (rock_2 material).*

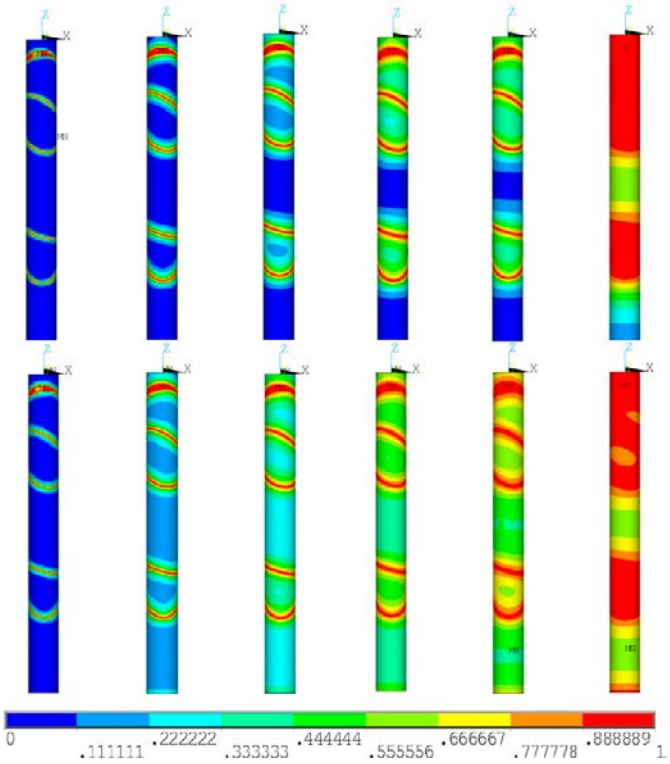

Figure A-13. *Distributions of degree of saturation for the borehole KO001701 with several fractures over time, ABOVE: bentonite hydration through the fractures only, BELOW: hydration through the fractures and rock-bentonite interface for the rock_1 rock matrix material (the same colour scale, different time).*

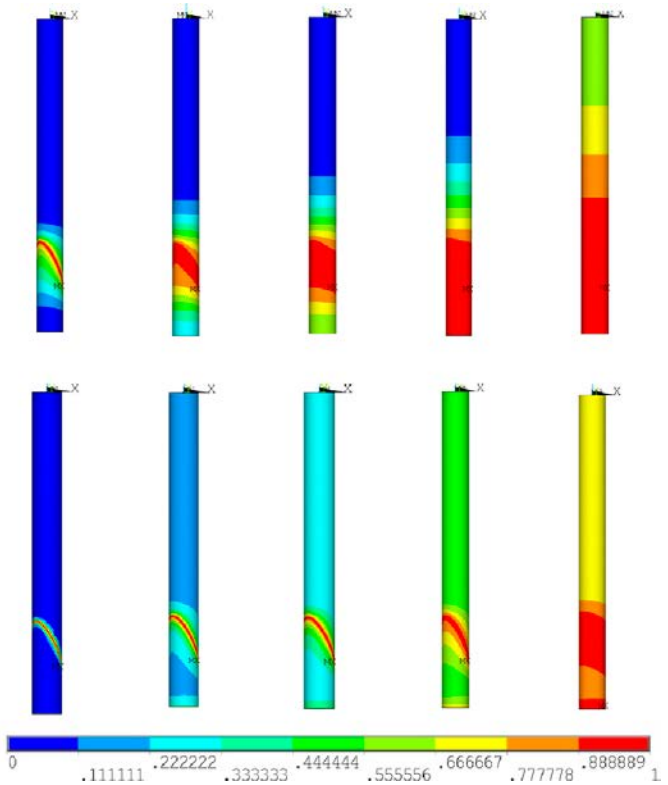

Figure A-14. *Distributions of degree of saturation for the borehole KO001701 with one fracture over time, ABOVE: bentonite hydration through the fracture only, BELOW: hydration through the fracture and rock-bentonite interface for the rock_1 rock matrix material (the same colour scale, different time).*

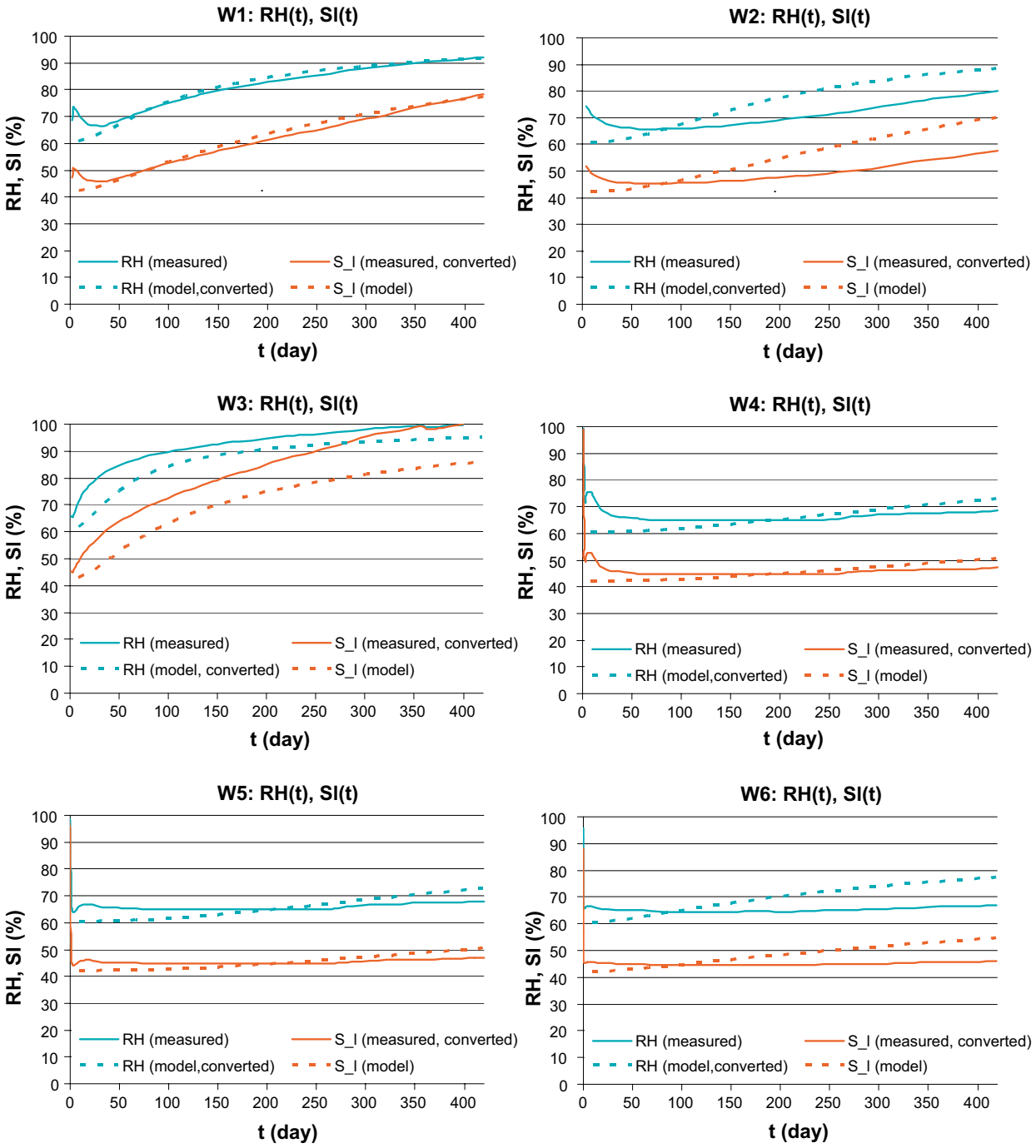

Figure A-15. *Relative humidity and degree of saturation for borehole KO0017G01 in comparison with measured data ("Rock 6" version with fracture aperture 2.3 cm).*

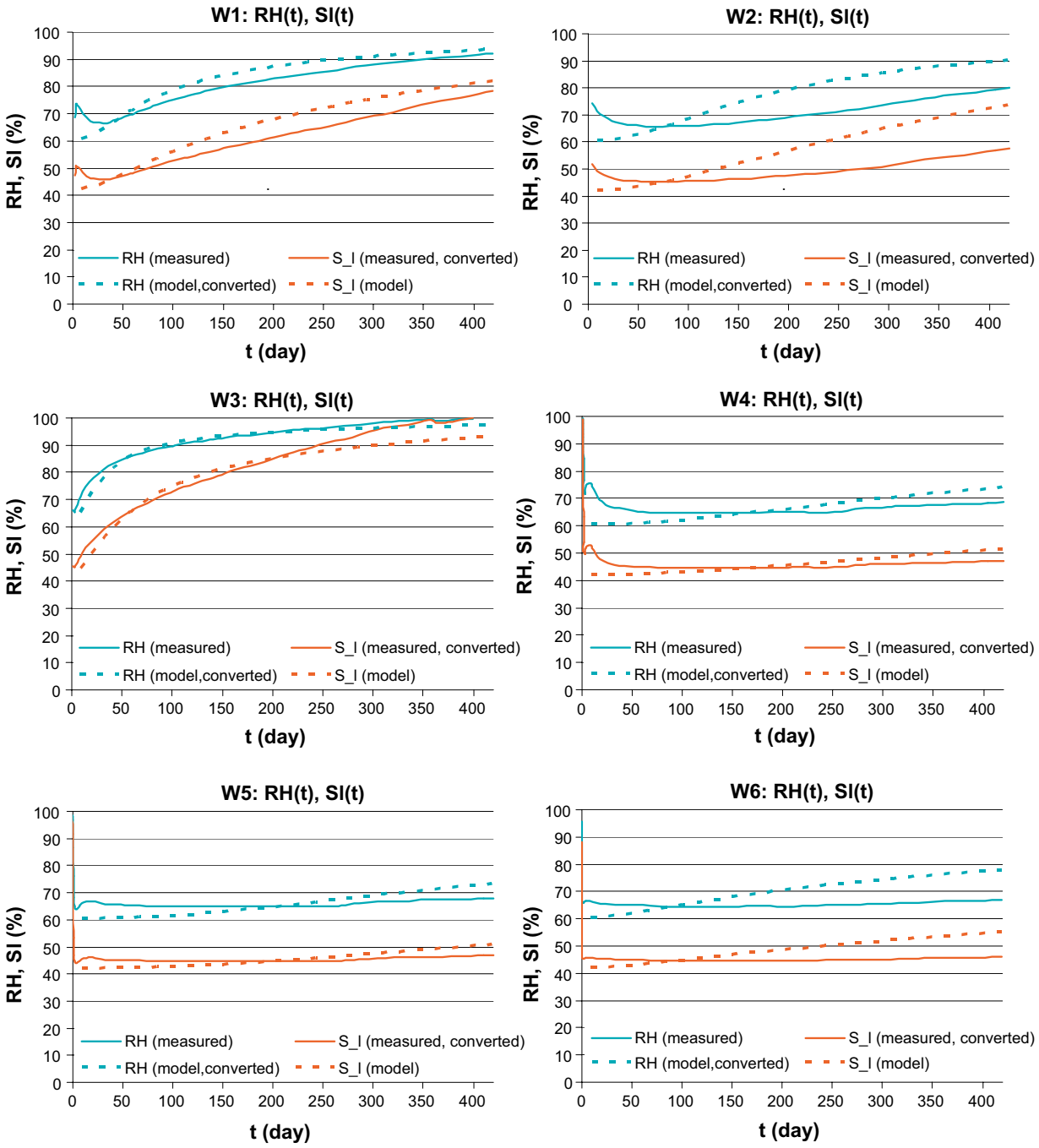

Figure A-16. *Relative humidity and degree of saturation for borehole KO0017G01 in comparison with measured data ("Rock 7" version with fracture aperture 4.6 cm).*

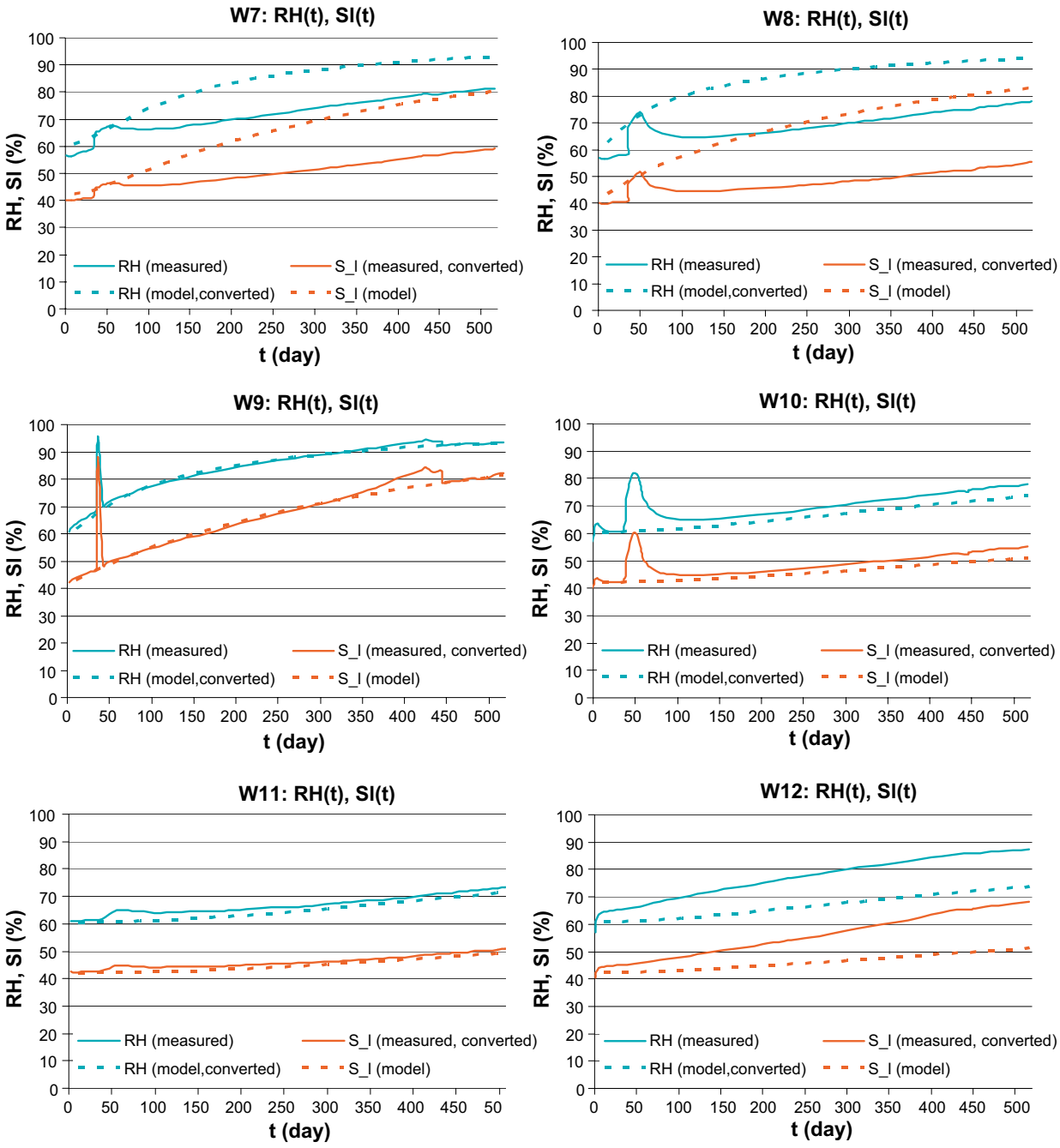

Figure A-17. *Relative humidity and degree of saturation for borehole KO0018G01 in comparison with measured data ("Rock 7" version with fracture aperture 1.2 cm).*

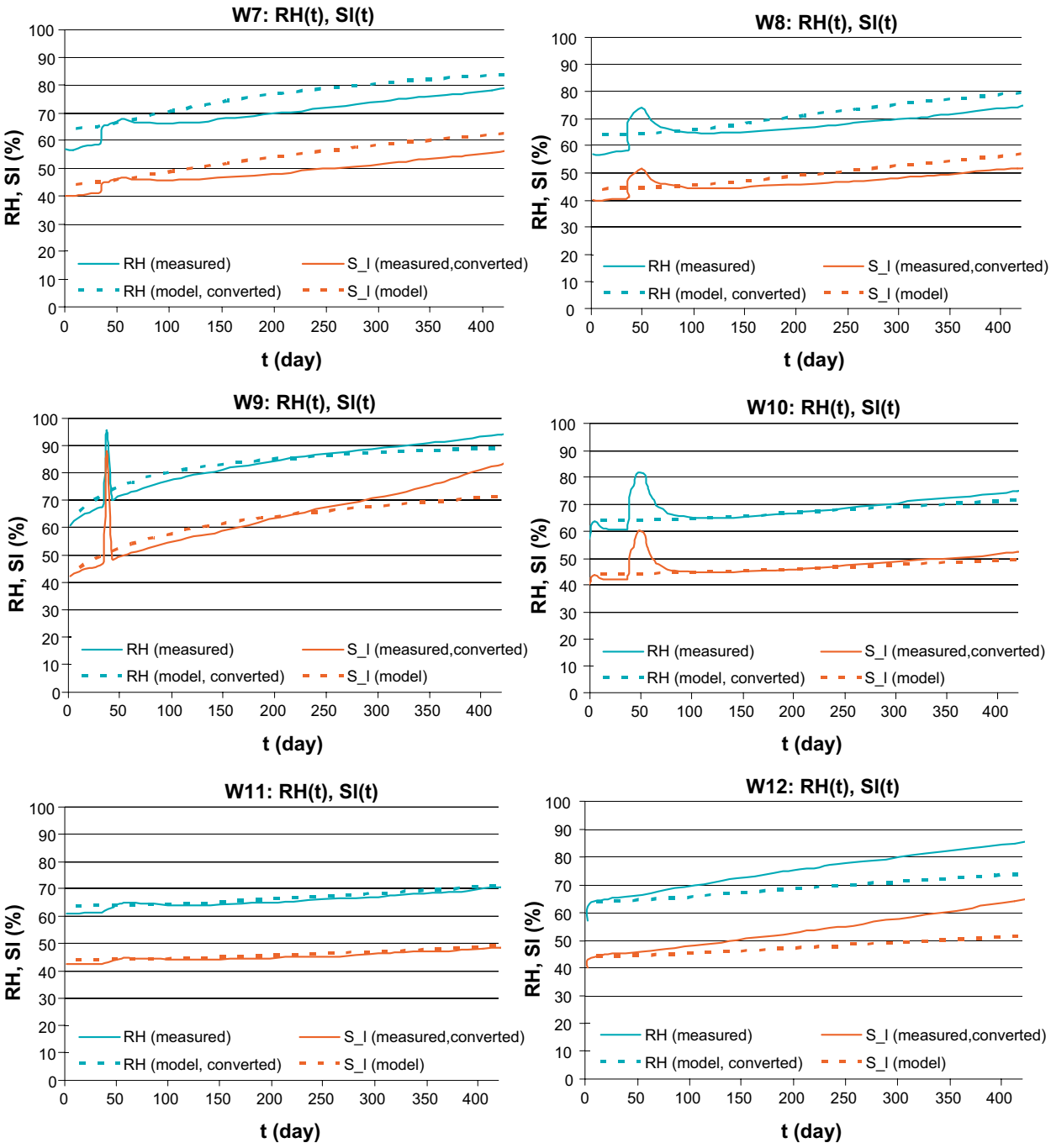

Figure A-18. *Relative humidity and degree of saturation for borehole KO0018G01 in comparison with measured data ("Rock 7" version with fracture aperture 1.2 cm and part of the fracture was set as impermeable).*

Table A-1. Time necessary to reach the different degrees of saturation for 3D models with fractures.

	Number of nodes	Number of elements
2D bentonite	621	1 024
2D bentonite + rock	11 969	23 249
3D boreholeKO0017G01 (5 fractures)	10 814	54 529
3D borehole KO0018G01 (6 fractures)	10 290	52 199
3D borehole KO0017G01 (1 fracture)	13 437	69 138
3D borehole KO0018G01 (1 fracture)	11 807	60 548

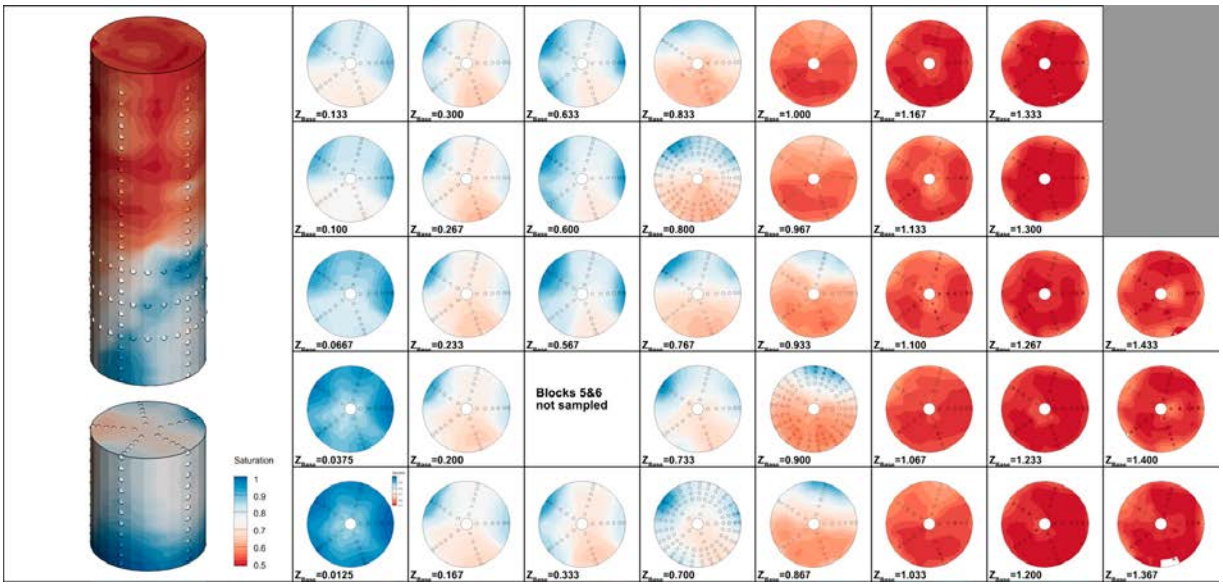

Figure A-19. *Degree of saturation – measured data for cross-section of borehole KO0017G01, adapted from Task 8 documentation.*

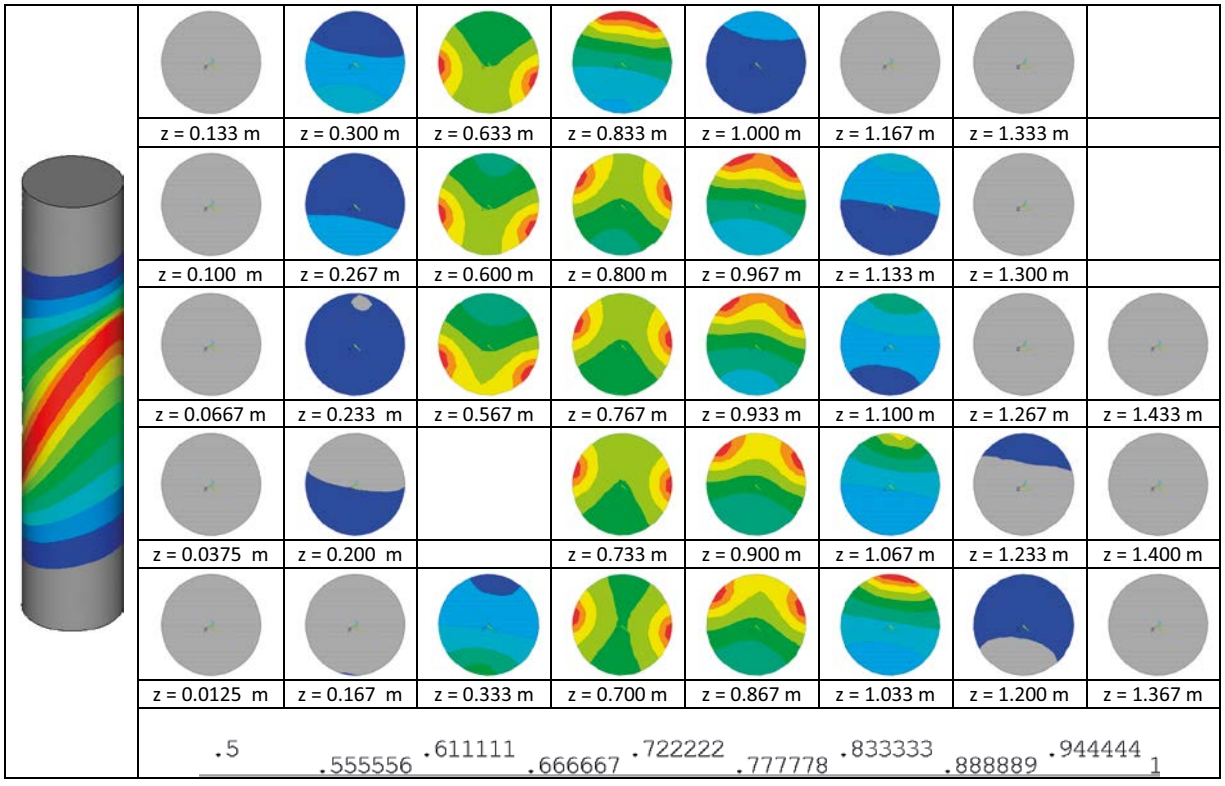

Figure A-20. *Degree of saturation – model data, cross-sections for borehole KO0017G01 – bottom part of the borehole (variant 6 with "Rock 5" boundary condition and 2.3 cm fracture aperture).*

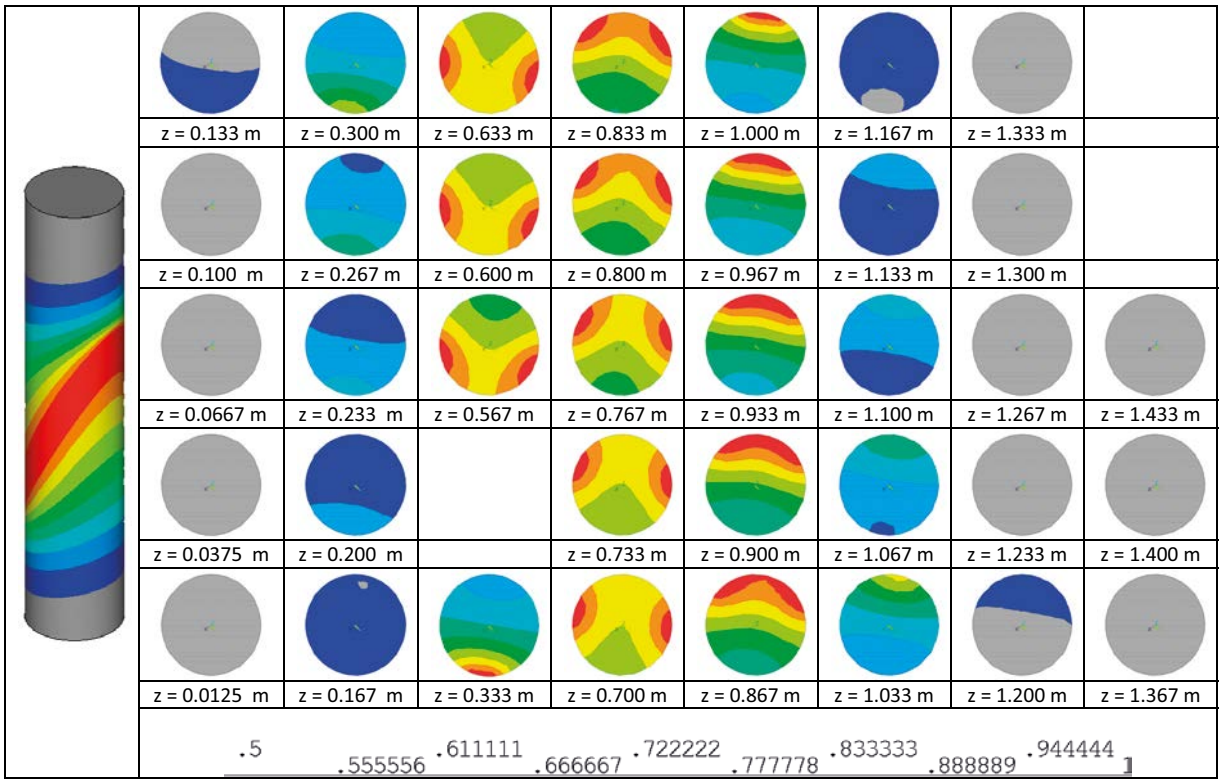

Figure A-21. *Degree of saturation – model data, cross-sections for borehole KO0017G01 – bottom part of the borehole (variant with "Rock 5" boundary condition with 4.6 cm fracture aperture).*

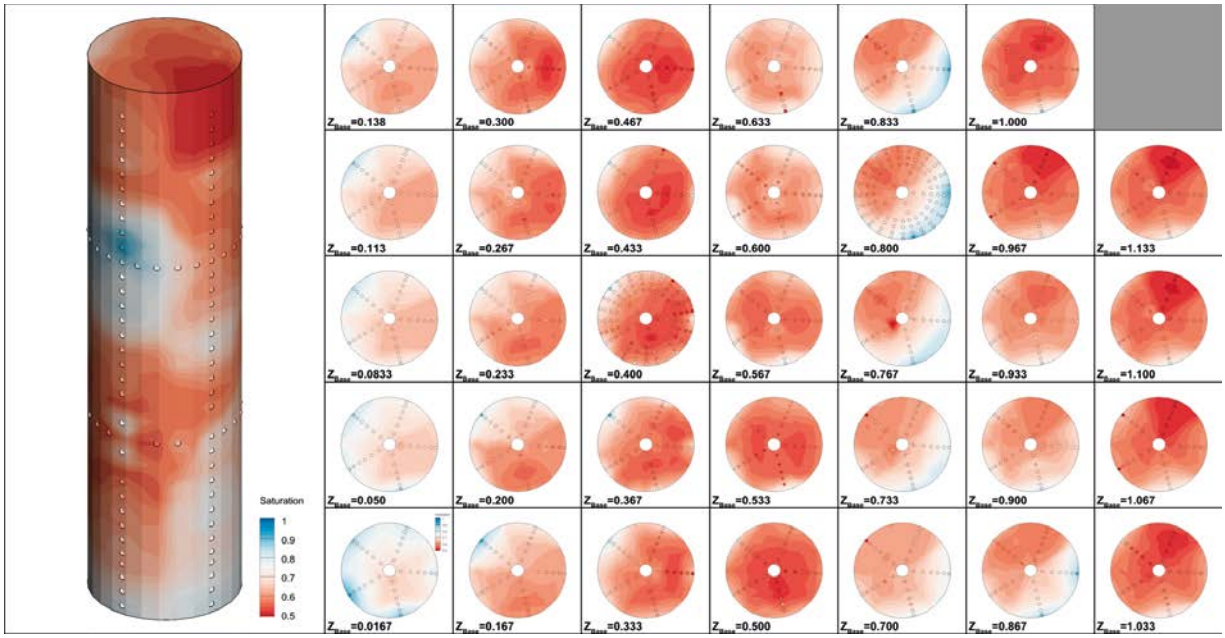

Figure A-22. *Degree of saturation – measured data for cross-section of borehole KO0018G01, adapted from Task 8 documentation.*

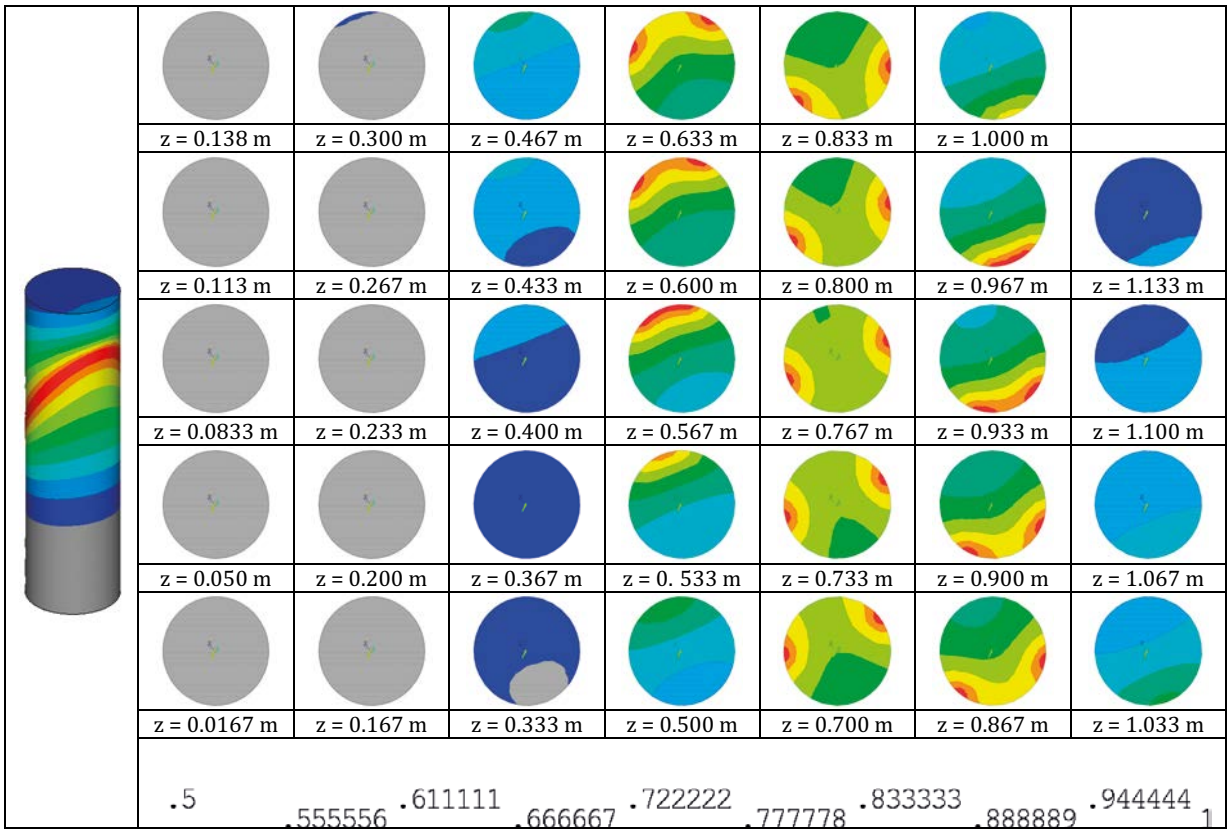

Figure A-23. *Degree of saturation – model data, cross-sections for borehole KO0018G01 – bottom part of the borehole (variant with "Rock 5" boundary condition with 1.17 cm fracture aperture).*

A-1 Modelling of water uptake test

Water Uptake Test was solved using the same model conception as all previous problems of Task 8 (diffusion equation with nonlinear diffusivity). Models were solved in four variant of diffusivity according to Table A-2 with different retention curves and relations for relative permeability. Used material parameters are referred in Table A-3.

Model geometry is shown in Figure A-24 and model results were compared with measured data.

We compared:

- Cumulative volume of water for all solved variants Figure A-25.
- Radial distribution of saturation for all solved models (in 107 and 203 days) – Figure A-26.
- Relative humidity in time for all solved model variants – Figure A-27.

Table A-2. Material models with different types of retention curve for Water Uptake Test modelling.

Retention curve	k_r	Diffusivity	Other parameters
van Genuchten	S_l^3	$D(S_l) = \frac{k}{n \cdot \mu} \cdot S_l^{\,3} \cdot \frac{P_0}{\lambda} \cdot (1-\lambda) \cdot \left(S_l^{\,-\frac{1}{\lambda}} - 1 \right)^{-\lambda} \cdot S_l^{\,\frac{-1-\lambda}{\lambda}}$	P_0 = 10 MPa λ = 0.28
	S_l^4	$D(S_l) = \frac{k}{n \cdot \mu} \cdot S_l^{\,3} \cdot \frac{P_0}{\lambda} \cdot (1-\lambda) \cdot \left(S_l^{\,-\frac{1}{\lambda}} - 1 \right)^{-\lambda} \cdot S_l^{\,\frac{-1-\lambda}{\lambda}}$	
Square law	S_l^3	$D(S_l) = \frac{k}{n \cdot \mu} \cdot 2 \cdot P_0$	P_0 = 19.3 MPa
	S_l^4	$D(S_l) = \frac{k}{n \cdot \mu} \cdot S_l \cdot 2 \cdot P_0$	

Table A-3. Material parameters applied in Water Uptake Test model.

Material parameters	
k [m^2]	6.4×10^{-21}
n [1]	0.44
ρ_{water} [$kg \times m^{-3}$]	1 000
μ_{water} [$Pa \times s$]	10^{-3}

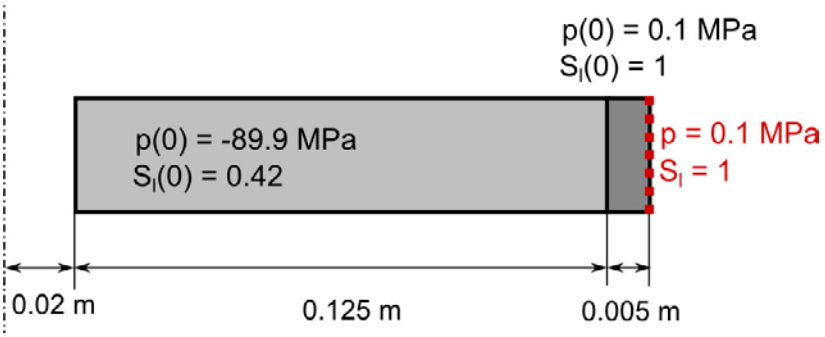

Figure A-24. *Geometry of axisymmetric model of Water Uptake Test and initial and boundary conditions.*

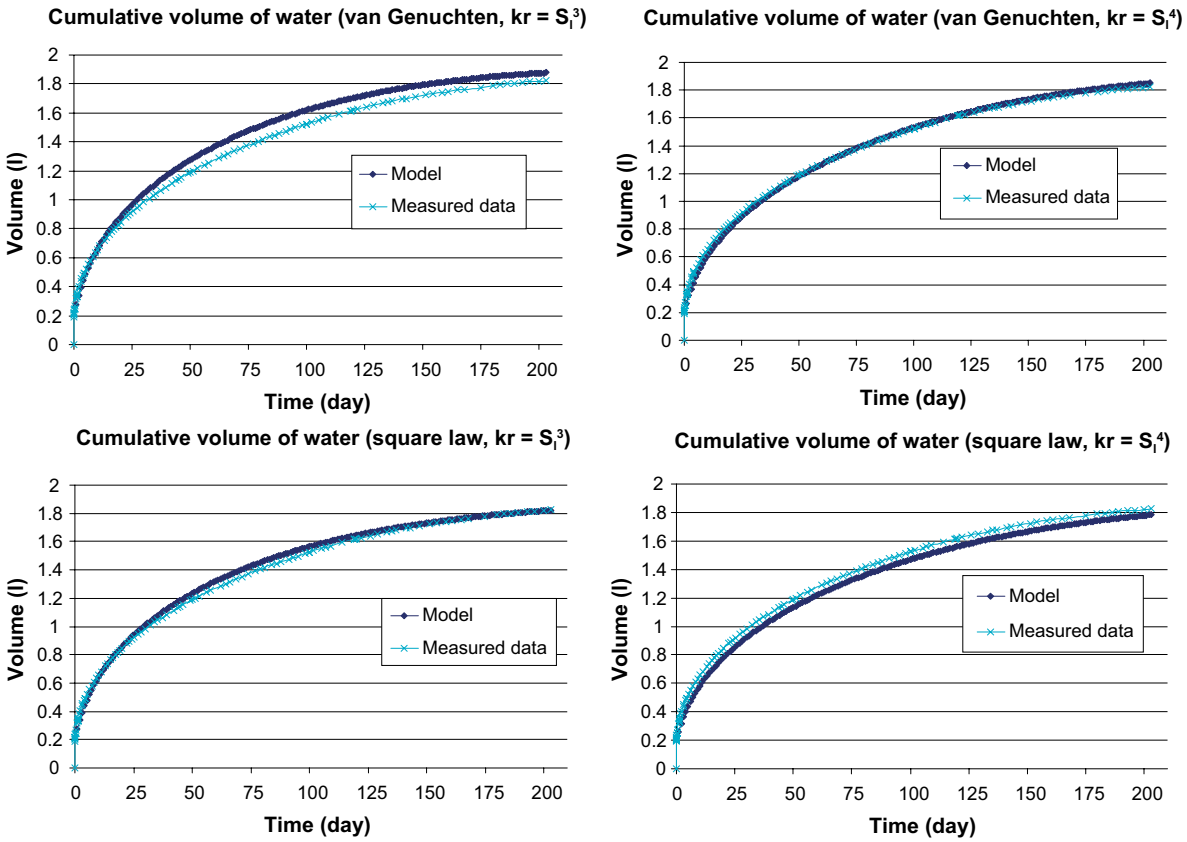

Figure A-25. *Cumulative volume of water for all solved variants in comparison with measured data (results of Water Uptake Test solved by diffusion equation with nonlinear diffusivity).*

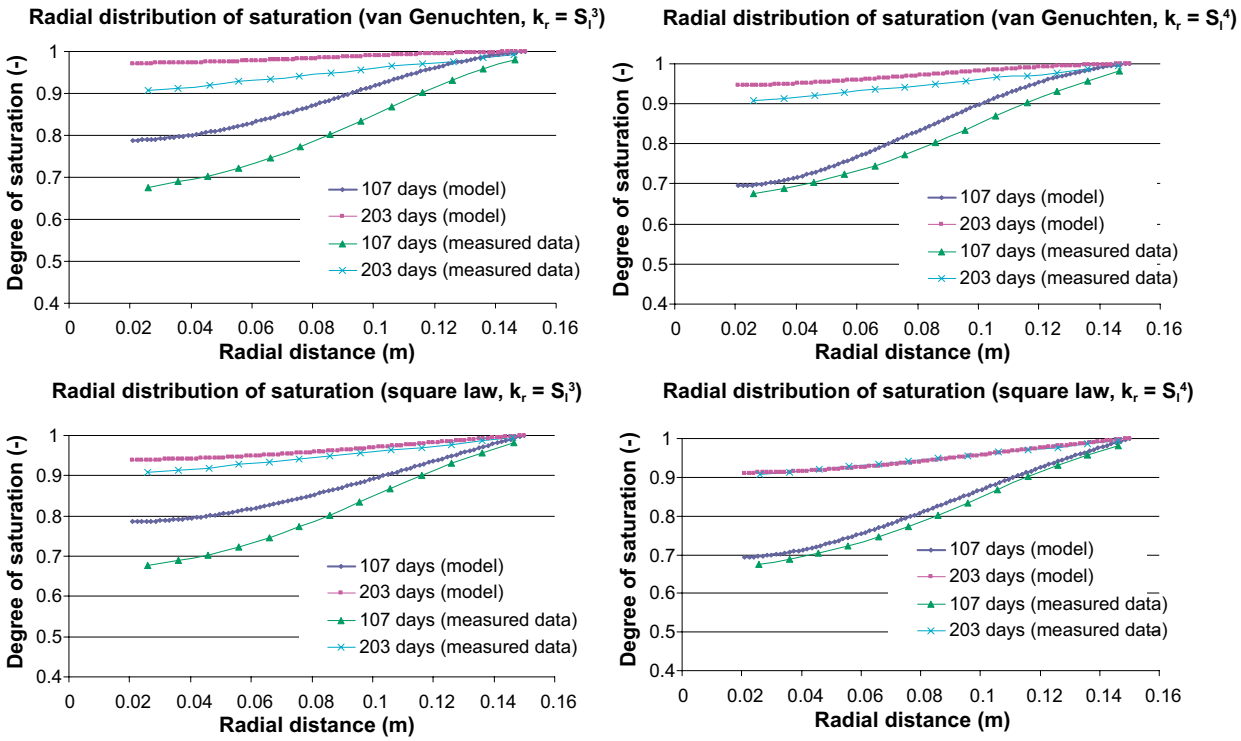

Figure A-26. *Radial distribution of saturation for all solved models (in 107 and 203 days) in comparison with measured data (results of Water Uptake Test solved by diffusion equation with nonlinear diffusivity).*

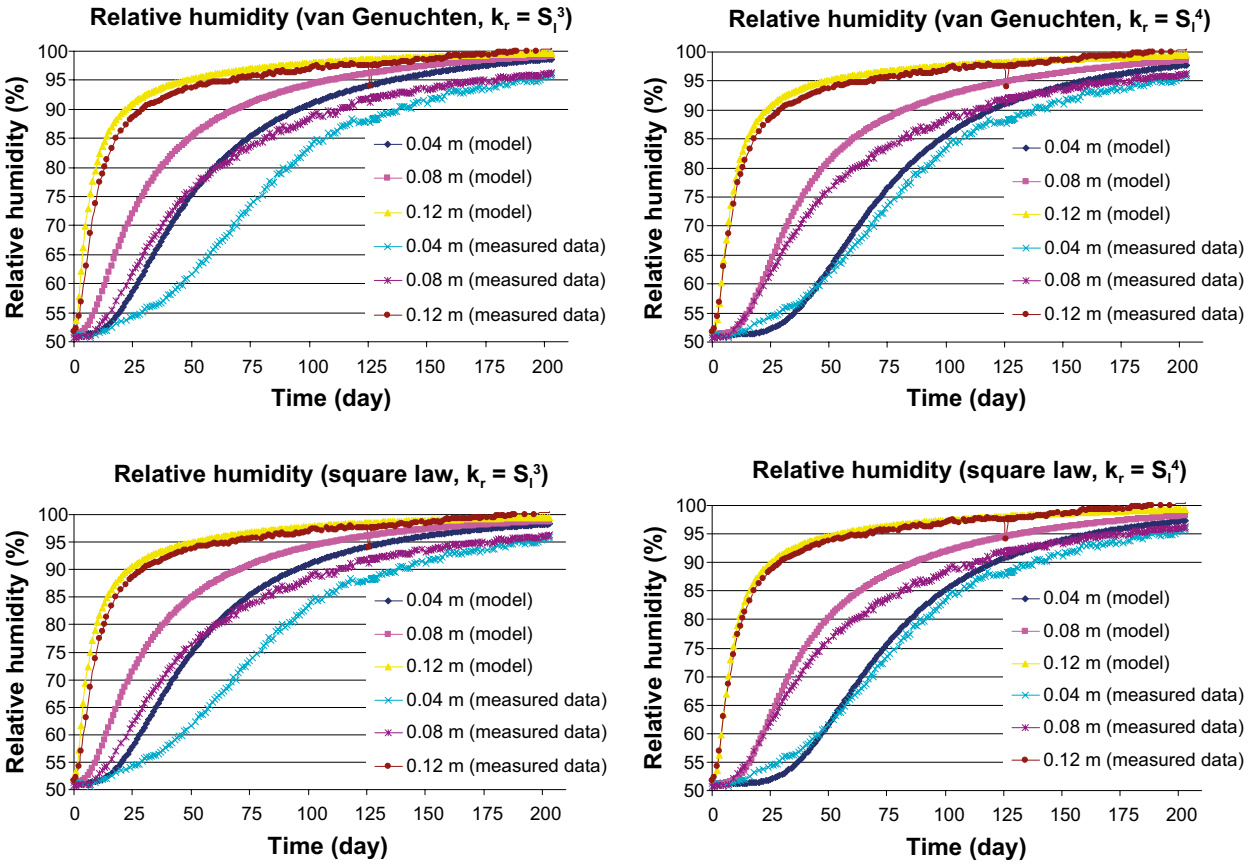

Figure A-27. *Relative humidity in time for all solved model variants in comparison with measured data (results of Water Uptake Test solved by diffusion equation with nonlinear diffusivity).*

Arkitektkopia AB, Bromma, 2018

SKB is responsible for managing spent nuclear fuel and radioactive waste produced by the Swedish nuclear power plants such that man and the environment are protected in the near and distant future.

skb.se